Pharmacological Research 175 (2022) 106037

Contents lists available at ScienceDirect

Pharmacological Research

journal homepage: www.elsevier.com/locate/yphrs

Review

# Properties of FDA-approved small molecule protein kinase inhibitors: A 2022 update☆

Robert Roskoski Jr.

*Blue Ridge Institute for Medical Research, 3754 Brevard Road, Suite 106, Box 19, Horse Shoe, NC 28742-8814, United States*

ARTICLE INFO

*Keywords:*
Catalytic spine
Hydrophobic interaction
Protein kinase inhibitor classification
Protein kinase structure
Regulatory spine
Shell residues

*Chemical compounds studied in this article:*
Belumosudil (PubChem CID: 11950170)
Cabozantinib (PubChem CID: 2510847)
Imatinib (PubChem CID: 5291)
Infigratinib (PubChem CID: 53235510)
Mobocertinib (PubChem CID: 118607832)
Sorafenib (PubChem CID: 216239)
Sunitinib (PubChem CID: 5329102)
Tepotinib (PubChem CID: 25171648)
Tivozanib (PubChem CID: 9911830)
Trilaciclib (PubChem CID: 68029832)

ABSTRACT

Owing to the dysregulation of protein kinase activity in many diseases including cancer, this enzyme family has become one of the most important drug targets in the 21st century. There are 68 FDA-approved therapeutic agents that target about two dozen different protein kinases and six of these drugs were approved in 2021. Of the approved drugs, twelve target protein-serine/threonine protein kinases, four are directed against dual specificity protein kinases (MEK1/2), thirteen block nonreceptor protein-tyrosine kinases, and 39 target receptor protein-tyrosine kinases. The data indicate that 58 of these drugs are prescribed for the treatment of neoplasms (49 against solid tumors including breast, lung, and colon, five against nonsolid tumors such as leukemias, and four against both solid and nonsolid tumors: acalabrutinib, ibrutinib, imatinib, and midostaurin). Three drugs (baricitinib, tofacitinib, upadacitinib) are used for the treatment of inflammatory diseases including rheumatoid arthritis. Of the 68 approved drugs, eighteen are used in the treatment of multiple diseases. The following six drugs received FDA approval in 2021 for the treatment of these specified diseases: belumosudil (graft vs. host disease), infigratinib (cholangiocarcinomas), mobocertinib and tepotinib (specific forms of non-small cell lung cancer), tivozanib (renal cell carcinoma), and trilaciclib (to decrease chemotherapy-induced myelosuppression). All of the FDA-approved drugs are orally effective with the exception of netarsudil, temsirolimus, and the newly approved trilaciclib. This review summarizes the physicochemical properties of all 68 FDA-approved small molecule protein kinase inhibitors including lipophilic efficiency and ligand efficiency.

## 1. The importance of therapeutic protein kinase inhibitors

Because of genetic alterations such as translocations and mutations as well as overexpression, the dysregulation of protein kinase activity is implicated in the pathogenesis of autoimmune, cardiovascular, inflammatory, and nervous diseases as well as number of neoplasms. As a consequence, protein kinases have become one of the most important drug targets in the 21st century [1,2]. Between 25% and 33% of the drug discovery efforts worldwide target these enzymes. The FDA approval of imatinib for the treatment of Philadelphia chromosome-positive chronic myelogenous leukemias in 2001 stimulated the pursuit of orally active therapeutic protein kinase inhibitors [3–5]. This revolutionary success was due to the imatinib inhibition of the active chimeric BCR-Abl protein-tyrosine kinase, which is the principal biochemical defect that produces these leukemias.

The more than five thousand protein kinase structures in the public domain facilitate structure-based drug development. Moreover, a larger number of proprietary structures within the pharmaceutical industry are used in the drug discovery process. About 180 orally effective protein kinase inhibitors are in clinical trials worldwide [6]. A complete listing of these agents, which is frequently updated, can be found at www.icoa.fr/pkidb/. There are 68 FDA-approved drugs that target more than 20 different protein kinases (see Supplementary material). Additional medicinals targeting these and other protein kinases are in clinical trials worldwide [4–7]. These protein kinases, however, represent only a small percentage of the 518-member protein kinase enzyme family.

*Abbreviations:* AS, activation segment; BP, back pocket; C-spine, catalytic spine; CS1, catalytic spine residue 1; CL, catalytic loop; EGFR, epidermal growth factor receptor; F, front pocket; FGFR, fibroblast growth factor receptor; GK, gatekeeper; GRL, glycine-rich loop; HGF, hepatocyte growth factor; KLIFS-3, kinase-ligand interaction fingerprint and structure residue-3; LE, ligand efficiency; LipE, lipophilic efficiency; MET, mesenchymal-epithelial transition factor receptor or hepatocyte growth factor receptor; NSCLC, non-small cell lung cancer; PDGFR, platelet-derived growth factor receptor; PKA, protein kinase A; Ro5, Lipinski's rule of five; R-spine, regulatory spine; RS1, regulatory spine residue 1; Sh2, shell residue 2; VEGFR, vascular endothelial growth factor receptor.

☆ This paper is dedicated to the memory of Dr. Phillip G. Schmid (1935-2021) – an early collaborator and friend.

*E-mail address:* rrj@brimr.org.

https://doi.org/10.1016/j.phrs.2021.106037
Received 10 December 2021; Accepted 12 December 2021
Available online 15 December 2021

The first comprehensive analysis performed by Manning et al. indicated that the human protein kinase lineage contains 478 typical and 40 atypical enzymes [8] such as phosphatidylinositol 3-kinase [5,9]. Protein kinases catalyze the following general reaction;.

$$MgATP^{1-} + \text{protein–O:H} \rightarrow \text{protein–O:}PO_3^{2-} + MgADP + H^+$$

Based upon the identity of the protein–OH groups, these catalysts are divided into protein-serine/threonine kinases (385), protein-tyrosine kinases (90 members), and protein-tyrosine kinase–like enzymes (43). The protein-tyrosine kinase collection includes both transmembrane receptor (58) and intracellular nonreceptor (32) proteins. Moreover, the protein kinase superfamily includes a small group of intracellular enzymes including MEK1/2 that mediate the phosphorylation of both tyrosine and then threonine residues within the activation segment of their target protein kinases; because of this unique action, MEK1/2 and related enzymes are called dual specificity protein kinases. Back-of-the-envelop calculations indicate that about one in every 40 human genes (518 protein kinase genes out of an estimated 20,000 human protein-encoding genes) encodes a protein kinase. Accordingly, protein kinases constitute about 2.5% of the human genome. Based upon a detailed study, Manning et al. reported that 244 protein kinases map to disease loci and cancer amplicons [8]. As new research is performed, such analyses predict a notable increase in the number of protein kinase therapeutic targets.

The US FDA has approved 68 small molecule therapeutic protein kinase antagonists as of 10 December 2021 (see Supplementary material), nearly all of which are orally effective with the exceptions of netarsudil (an eye drop) and temsirolimus and the newly approved trilaciclib (which are given intravenously). Ruxolitinib is an orally effective JAK1/2 protein kinase blocker that was approved for the treatment of myelofibrosis and polycythemia vera in 2011. The drug is topically active as a creme and was approved in 2021 for the treatment of atopic dermatitis. Of the 68 approved drugs, twelve target protein-serine/threonine protein kinases, four are directed against dual specificity protein kinases (MEK1/2), thirteen block nonreceptor protein-tyrosine kinases, and 39 target receptor protein-tyrosine kinases (Table 1). The data indicate that 58 of these drugs are prescribed for the treatment of neoplasms (49 against solid tumors such as breast, colon, and lung, five against nonsolid tumors such as leukemias, and four against both types of tumors: acalabrutinib, ibrutinib, imatinib, and midostaurin). Three drugs are used in the treatment of rheumatoid arthritis (baricitinib, tofacitinib, upadacitinib) and two drugs are approved for the treatment of graft vs. host disease (ibrutinib, belumosudil). At least 25 of the approved medications are multikinase antagonists. Because the specificity of many of these drugs is unknown, it is probable that many more of the approved medicinals are multikinase inhibitors. The blockade of multiple kinases has potential advantages and disadvantages. For example, the therapeutic efficacy of multikinase inhibitors may be related to the inhibition of two or more targets. For instance, sunitinib and cabozantinib have potent off-target activity against the Axl receptor protein-tyrosine kinase and this engagement may add to their clinical effectiveness [13]. Contrariwise, the blockade of off-target kinases may lead to various side effects and contribute to adverse events. Consequently, we have the quandary of whether a magic shotgun is to be preferred over Paul Ehrlich's magic bullet (zauberkugel) [14].

Nine of the FDA-approved protein kinase blockers are used for the treatment of nonneoplastic diseases. For example, fedratinib is prescribed for the treatment of myelofibrosis, netarsudil is employed for the treatment of glaucoma, sirolimus and belumosudil are exploited for the treatment of graft vs. host disease, nintedanib is used for the treatment of idiopathic pulmonary fibrosis, ruxolitinib is used for the treatment of myelofibrosis, fostamatinib is prescribed for the treatment of chronic immune thrombocytopenia and polycythemia vera, tofacitinib is used for the treatment of rheumatoid arthritis, Crohn disease, and ulcerative colitis, and baricitinib and upadacitinib are employed for the treatment

**Table 1**
FDA-approved small molecule protein kinase inhibitors, their protein kinase targets, and therapeutic indications[c].

| Drug (Code) Trade name | Year approved | Primary targets[a] | Therapeutic indications[b] |
|---|---|---|---|
| Abemaciclib (LY2835219) Verzenio | 2017 | CDK4/6 | Combination therapy with an (i) aromatase inhibitor or with (ii) fulvestrant or as a monotherapy for breast cancers |
| Acalabrutinib (ACP-196) Calquence | 2017 | BTK | Mantle cell lymphomas, CLL, SLL |
| Afatinib (BIBW 2992) Tovok | 2013 | ErbB1/2/4 | NSCLC |
| Alectinib (CH5424802) Alecensa | 2015 | ALK, RET | ALK-positive NSCLC |
| Avapritinib (BLU285) Ayvakit | 2020 | PDGFRα | GIST with *PDGFRα* exon 18 mutation |
| Axitinib (AG-013736) Inlyta | 2012 | VEGFR1/2/3 | RCC |
| Baricitinib (LY 3009104) Olumiant | 2018 | JAK1/2 | Rheumatoid arthritis |
| **Belumosudil** (KD025) Rezurock | 2021 | ROCK2 | Graft vs. host disease |
| Binimetinib (MEK162) Mektovi | 2018 | MEK1/2 | Combination therapy with encorafenib for $BRAF^{V600E/K}$ melanomas |
| Bosutinib (SKI-606) Bosulif | 2012 | BCR-Abl | CML |
| Brigatinib (AP 26113) Alunbrig | 2017 | ALK | ALK-positive NSCLC |
| Cabozantinib (BMS-907351) Cometriq | 2012 | RET, VEGFR2 | Medullary thyroid cancers, RCC, HCC |
| Capmatinib (INC-280) Tabrecta | 2020 | MET | NSCLC with MET exon 14 skipping |
| Ceritinib (LDK378) Zykadia | 2014 | ALK | ALK-positive NSCLC resistant to crizotinib |
| Cobimetinib (GDC-0973) Cotellic | 2015 | MEK1/2 | $BRAF^{V600E/K}$ melanomas in combination with vemurafenib |
| Crizotinib (PF 2341066) Xalkori | 2011 | ALK, ROS1 | ALK or ROS1-postive NSCLC |
| Dabrafenib (GSK2118436) Tafinlar | 2013 | B-Raf | $BRAF^{V600E/K}$ melanomas, $BRAF^{V600E}$ NSCLC, $BRAF^{V600E}$ anaplastic thyroid cancers |
| Dacomitinib (PF-00299804) Visimpro | 2018 | EGFR | *EGFR*-mutant NSCLC |
| Dasatinib (BMS-354825) Sprycell | 2006 | BCR-Abl | CML |
| Encorafenib (LGX818) Braftovi | 2018 | B-Raf | Combination therapy with binimetinib for $BRAF^{V600E/K}$ melanomas |
| Entrectinib (RXDX-101) Rozlytrek | 2019 | TRKA/B/C, ROS1 | Solid tumors with NTRK fusion proteins, ROS1-positive NSCLC |
| Erdafitinib (JNJ-42756493) Balversa | 2019 | FGFR1/2/3/4 | Urothelial bladder cancers |
| Erlotinib (OSI-774) Tarceva | 2004 | EGFR | NSCLC, pancreatic cancers |
| Everolimus (RAD001) Afinitor | 2009 | FKBP12/mTOR | HER2-negative breast cancers, pancreatic neuroendocrine tumors, RCC, angiomyolipomas, subependymal giant cell astrocytomas |
| | 2019 | JAK2 | Myelofibrosis |

(*continued on next page*)

**Table 1** (*continued*)

| Drug (Code) Trade name | Year approved | Primary targets[a] | Therapeutic indications[b] |
|---|---|---|---|
| Fedratinib (TG101348) Inrebic | 2018 | Syk | Chronic immune thrombocytopenia |
| Fostamatinib (R788) Tavalisse | 2003 | EGFR | NSCLC |
| Gefitinib (ZD1839) Iressa | 2018 | Flt3 | AML |
| Gilteritinib (ASP2215) Xospata | 2013 | BTK | CLL, mantle cell lymphomas, marginal zone lymphomas, graft vs. host disease, Waldenström macroglobulinemia |
| Ibrutinib (PCI-32765) Imbruvica | 2001 | BCR-Abl | $Ph^+$ CML or ALL, aggressive systemic mastocytosis, chronic eosinophilic leukemias, dermatofibrosarcoma protuberans, hypereosinophilic syndrome, GIST, myelodysplastic/ myeloproliferative disease |
| Imatinib (STI571) Gleevec | 2021 | FGFR2 | Cholangiocarcinomas with FGFR2 fusion proteins |
| **Infigratinib** (BGJ 398) Truseltiq | 2007 | EGFR, ErbB2/ HER2 | HER2-positive breast cancers |
| Lapatinib (GW572016) Tykerb | 2018 | TRKA/B/ C | Solid tumors with NTRK fusion proteins |
| Larotrectinib (LOXO-101) Vitrakvi | 2015 | VEGFR, RET | Differentiated thyroid cancers |
| Lenvatinib (AK175809) Lenvima | 2018 | ALK | ALK-positive NSCLC |
| Lorlatinib (PF-06463922) Lorbrena | 2017 | Flt3 | AML, mastocytosis, mast cell leukemias |
| Midostaurin (CPG 41251) Rydapt | 2021 | EGFR | NSCLC for EGFR-positive exon 21 insertions |
| **Mobocertinib** (TAK-788) Exkivity | 2017 | ErbB2/ HER2 | HER2-positive breast cancers |
| Neratinib (HKI-272) Nerlynx | 2018 | ROCK1/2 | Glaucoma |
| Netarsudil (AR11324) Rhopressa | 2007 | BCR-Abl | $Ph^+$ CML |
| Nilotinib (AMN107) Tasigna | 2014 | FGFR1/2/ 3 | Idiopathic pulmonary fibrosis |
| Nintedanib (BIBF-1120) Vargatef | 2015 | EGFR T970M | NSCLC |
| Osimertinib (AZD-9292) Tagrisso | 2015 | CDK4/6 | Estrogen receptor- and HER2-positive breast cancers |
| Palbociclib (PD-0332991) Ibrance | 2009 | VEGFR1/ 2/3 | RCC, soft tissue sarcomas |
| Pazopanib (GW786034) Votrient | 2020 | FGFR2 | Advanced cholangiocarcinoma with a FGFR2 fusion or rearrangement |
| Pemigatinib (INCB054828) Pemazyre | 2019 | CSF1R | Tenosynovial giant cell tumors |
| Pexidartinib (PLX3397) Turalio | 2012 | BCR-Abl | $Ph^+$ CML or ALL |
| Ponatinib (AP 24534) Iclusig | 2020 | RET | RET-fusion (i) NSCLC, (ii) medullary thyroid cancer, (iii) thyroid cancer |
| Pralsetinib (Blu-667) Gavreto | 2012 | VEGFR1/ 2/3 | Colorectal cancers |
| Regorafenib (BAY 734506) Stivarga | 2018 | Syk | |

**Table 1** (*continued*)

| Drug (Code) Trade name | Year approved | Primary targets[a] | Therapeutic indications[b] |
|---|---|---|---|
| R406 (active metabolite of fostamatinib) | | | Chronic immune thrombocytopenia |
| Ribociclib (LEE011) Kisqali | 2017 | CDK4/6 | Combination therapy with an aromatase inhibitor for breast cancers |
| Ripretinib (DCC-2618) Qinlock | 2020 | Kit, PDGFRα | Fourth-line treatment for GIST |
| Ruxolitinib (INCB-018424) Jakafi | 2011 | JAK1/2/ 3,Tyk | Myelofibrosis, polycythemia vera, atopic dermatitis |
| Selpercatinib (CEGM9YBNG) Retevmo | 2020 | RET | RET fusion NSCLC and thyroid cancers and *RET* mutant medullary thyroid cancers |
| Selumetinib (AZD6224) Koselugo | 2020 | MEK1/2 | Neurofibromatosis type I |
| Sirolimus (AY 22989) Rapamycin | 1999 | FKBP12/ mTOR | Kidney transplants, lymphangioleiomyomatosis |
| Sorafenib (BAY 43–9006) Nexavar | 2005 | VEGFR1/ 2/3 | HCC, RCC, thyroid cancer (differentiated) |
| Sunitinib (SU11248) Sutent | 2006 | VEGFR2 | GIST, pancreatic neuroendocrine tumors, RCC |
| Temsirolimus (CCI-779) Torisel | 2007 | FKBP12/ mTOR | RCC |
| **Tepotinib** (EMD 1214063) Tepmetko | 2021 | MET | NSCLC with *MET* mutations |
| **Tivozanib** (AV951) Fotvida | 2021 | VEGFR2 | Third-line treatment of RCC |
| Tofacitinib (CP-690550) Tasocitinib | 2012 | JAK3 | Rheumatoid arthritis, psoriatic arthritis, ulcertive colitis |
| Trametinib (GSK1120212) Mekinist | 2013 | MEK1/2 | $BRAF^{V600E/K}$ melanomas, $BRAF^{V600E}$ NSCLC |
| **Trilaciclib** (G1T28) Cosela | 2021 | CDK4/6 | Chemotherapy-induced myelosuppression |
| Tucatinib (ONT-380) Tukysa | 2020 | ErbB2/ HER2 | Combination second-line treatment for HER2-positive breast cancers |
| Upadacitinib (ABT-494) Rinvoq | 2019 | JAK1 | Second-line treatment for rheumatoid arthritis |
| Vandetanib (ZD6474) Zactima | 2011 | VEGFR2 | Medullary thyroid cancers |
| Vemurafenib (PLX-4032) Zelboraf | 2011 | B-Raf | $BRAF^{V600E}$ melanomas |
| Zanubrutinib (BGB3111) Brukinsa | 2019 | BTK | Mantle cell lymphomas |

[a] Although many of these drugs are multikinase inhibitors, only the primary therapeutic targets are given here.

[b] ALL, acute lymphoblastic leukemias; AML, acute myelogenous leukemias; CLL, chronic lymphocytic leukemias; CML, chronic myelogenous leukemias; ErbB2/HER2, human epidermal growth factor receptor-2; GIST, gastrointestinal stromal tumors; HCC, hepatocellular carcinomas; NSCLC, non-small cell lung cancers; $Ph^+$, Philadelphia chromosome positive; RCC, renal cell carcinomas; SLL, small lymphocytic lymphomas.

[c] Drugs not previously reviewed in Refs. [10–12] are given in bold type.

of rheumatoid arthritis [10–12]. Furthermore, ibrutinib and sirolimus are used for the treatment of both neoplastic and nonneoplastic diseases.

The list of FDA-approved kinase inhibitors includes eight drugs that form covalent bonds with their target enzymes and they are classified as TCIs (targeted covalent inhibitors) [15]. These include neratinib (targeting ErbB2 in HER2-positive breast cancers), osimertinib (blocking

*EGFR T970M* mutants in NSCLC), acalabrutinib (inhibiting BTK in mantle cell lymphomas), afatinib (targeting EGFR in NSCLC), ibrutinib (blocking BTK in chronic lymphocytic leukemias, mantle cell lymphomas, marginal zone lymphomas, chronic graft vs. host disease, and Waldenström macroglobulinemia), dacomitinib (inhibiting mutant *EGFR* in lung cancers), newly approved mobocertinib (targeting *EGFR* with exon 20 insertions in NSCLC) and zanubrutinib (targeting BTK in mantle cell lymphomas). The closely related *EGFR* and *ErbB4* of the ErbB1/2/3/4 epidermal growth factor receptor family are the most frequently mutated protein kinases in all cancers [3]. For a tally of the properties of small molecule protein kinase antagonists that were approved by the FDA prior to 2021, see Refs. [10–12].

Of the 68 FDA-approved protein kinase inhibitors, eighteen are used in the treatment of more than one disease. Imatinib, for example, is approved for the treatment of eight distinct illnesses (Table 1). This agent inhibits the nonreceptor protein-tyrosine kinase Abl (and the BCR-Abl chimera – responsible for the pathogenesis of chronic myelogenous leukemias), Abl2, epithelial discoidin domain-containing receptor-1 (DDR1) and receptor-2 (DDR2), Kit (the stem cell factor receptor), and PDGFRα/β. DDR1/2 are activated by collagen and they participate in cell differentiation, migration, proliferation, and remodeling the extracellular matrix. Imatinib is FDA-approved for (i) the first-line treatment of Philadelphia chromosome-positive chronic myelogenous leukemias, (ii) *KIT* mutation-positive gastrointestinal stromal tumors, (iii) dermatofibrosarcoma protuberans, (iv) chronic eosinophilic leukemias, (v) acute lymphoblastic leukemias (vi) myelodysplastic/myeloproliferative diseases with *PDGFR* gene-rearrangements, (vii) hypereosinophilic syndrome, and (viii) as a second-line treatment for aggressive systemic mastocytosis without the *KIT* $^{D816V}$ mutation [2,10]. Imatinib is used off-label for desmoid tumors, chordomas, advanced *KIT*-mutant melanomas, and the treatment of chronic myelogenous leukemias following allogeneic stem cell transplantation. Imatinib is thus a broad-spectrum inhibitor.

## 2. Protein kinase structure and mechanism

### 2.1. Primary, secondary, and tertiary structures

The newly approved drugs described in this review interact with several protein kinases including the protein-serine/threonine kinases ROCK2 and CDK4/6 and the receptor protein-tyrosine kinases FGFR1/2/3/4, ErbB1/2/3/4, MET, and VEGFR1/2/3 so that the following description is generic. As initially described for PKA (protein kinase A) by Knighton et al., protein kinases possess a small N-terminal lobe and large C-terminal lobe (Fig. 1) [16]. The amino-terminal lobe is made up of a five-stranded antiparallel β-sheet (β1–β5) and an αC-helix that

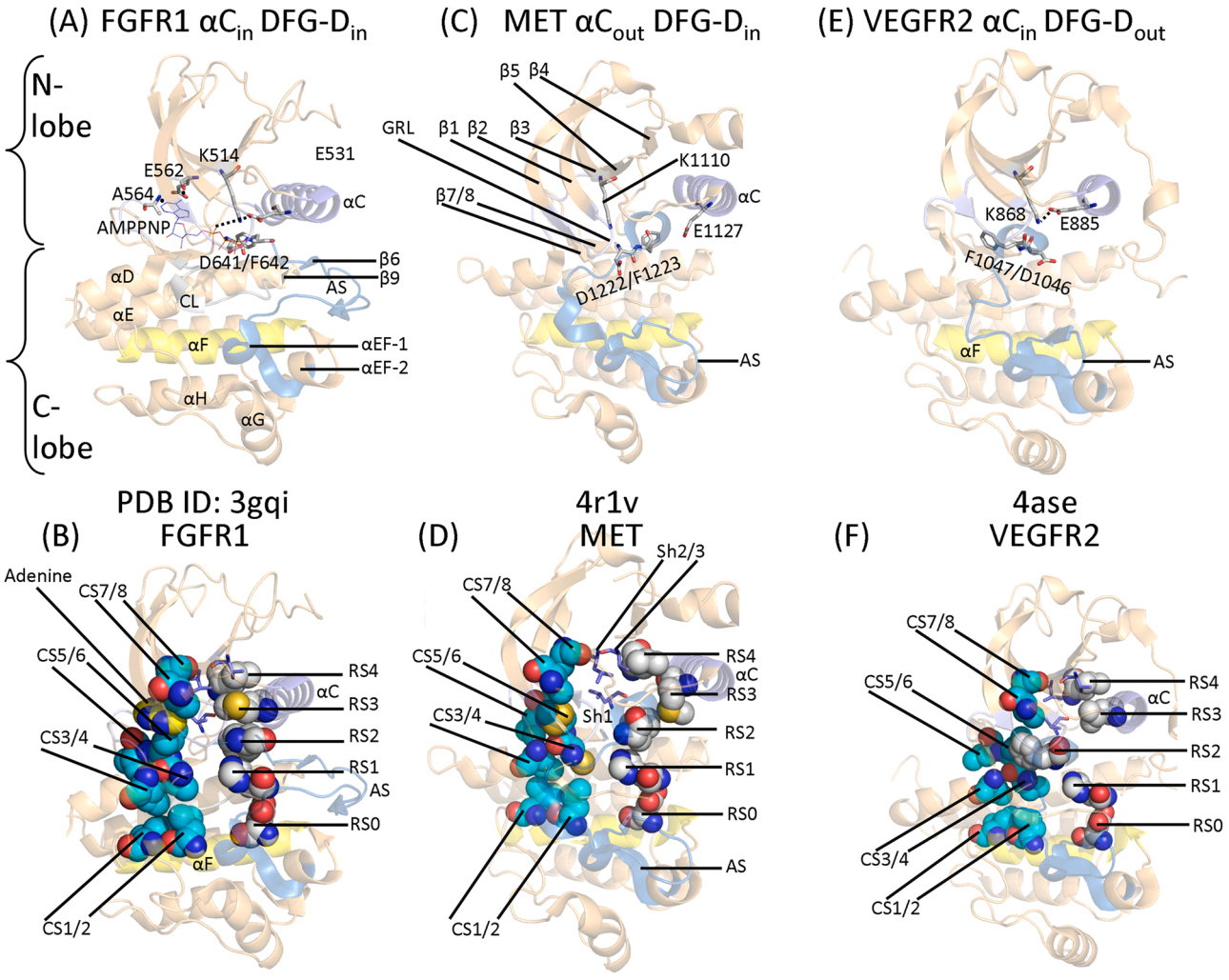


**Fig. 1.** (A) Overview of active FGFR1 with bound AMP-PNP (adenylyl imidodiphosphate) and (B) its C-spine and R-spine residues. (C) The αC$_{out}$ and DFG-D$_{in}$ structure of dormant MET and (D) its C-spine, R-spine, and shell residues. (E) Overview of the DGF-D$_{out}$ αC$_{in}$ structure of VEGFR2 and (F) its C-spine and R-spine residues. AS, activation segment; CL, catalytic loop; GRL, glycine-rich loop. Figs. 1, 2, 3, and 5 were prepared using the PyMOL Molecular Graphics System Version 1.5.0.4 Schrödinger, LLC.

occurs in active and inactive orientations [17,18]. The small lobe contains a glycine-rich loop (GRL), sometimes called the P-loop (for phosphate), which links the β1- and β2-strands; the loop consists of GxGxΦGV where the Φ denotes a hydrophobic residue. The valine following the G-rich segment makes hydrophobic contact with the adenine moiety of ATP as well as several small molecule protein kinase antagonists. Protein kinases contain an AxK sequence within the β3-strand and an invariant glutamate near the middle of the αC-helix. An ionic bond occurs between the positively charged β3-strand lysine (K) and the negatively charged αC-glutamate (E) in catalytically active protein kinases and this structure corresponds to the "$\alpha C_{in}$" conformation (Fig. 1A). The $\alpha C_{in}$ conformation is necessary, but not sufficient, for the expression of full enzyme activity. Furthermore, the absence of this ionic bond indicates that the enzyme is catalytically inactive and the resulting structure corresponds to the "$\alpha C_{out}$" conformation (Fig. 1C). The conversion of the $\alpha C_{out}$ structure to the $\alpha C_{in}$ conformation is required for catalytic activity.

The carboxyterminal lobe is mostly α-helical with eight conserved helices (αD–αI, αEF1, αEF2) [19]. The C-terminal lobe of active protein kinases also contains four short β-strands (β6–β9). The second amino acid residue of the β7-strand, which makes up the floor of the adenine binding pocket, interacts hydrophobically with all known ATP-competitive protein kinase inhibitors [20]. The large lobe contains a catalytic loop (CL) that participates in the transfer of the γ-phosphoryl group from ATP to the protein kinase substrates. The large lobe also places the protein/peptide substrate into the active site to enable catalysis.

Hanks and Hunter described 12 subdomains (I–VIa, VIb–XI) that constitute the working core of protein kinases [21]. A K/E/D/D (Lys/-Glu/Asp/Asp) tetrad plays a central role in the catalytic activity of all protein kinases. The *K* of the tetrad is the lysine of the β3-strand that forms ionic bonds with (i) the αC-helix glutamate to form the $\alpha C_{in}$ structure, (ii) the α-phosphate, and (iii) the β-phosphate (not shown) of ATP. Residues within the activation segment position the phosphorylatable substrate in the active site. Furthermore, the catalytic-loop HRD-aspartate (the first *D* of the K/E/*D*/D tetrad), which functions as a Lowry-Brönsted base (proton acceptor), performs an essential role during catalysis. Madhusudan et al. hypothesized that the HRD-aspartate of the catalytic loop abstracts the proton from the protein substrate –OH [22]. Moreover, Zhou and Adams suggested that the HRD-aspartate positions the hydroxyl group of the protein substrate to promote an in-line nucleophilic attack of the oxygen with the γ-phosphate of ATP [23]. See Ref. [24] for a comprehensive summary of protein kinase enzymology and see Table 2 for a list of the important residues in selected protein kinase targets considered in this paper.

The second *D* of the K/E/D/*D* tetrad corresponds to the first residue of the protein-substrate-binding activation segment. This segment of all protein kinases begins with DFG and ends with APE or a similar triad. Activation segments, which are important structural and regulatory components of all protein kinases, are about 35–40 residues long [25]. The catalytic loop of protein kinases is made up of an $HRD(x)_4N$ signature. The primary structure of the activation segment occurs on the C-terminal side of the catalytic loop. Two $Mg^{2+}$ ions – $Mg^{2+}(1)$ and $Mg^{2+}(2)$ – are required for the catalytic activity of almost all protein kinases. $Mg^{2+}(1)$ interacts with DFG-D of the activation segment and $Mg^{2+}(2)$ interacts with the asparagine (N) at the end of the catalytic loop (not shown).

The primary structure and length of the middle region of the activation segment vary greatly among the protein kinase superfamily [2]. The activation segment of nearly all members of the protein kinase superfamily contains one or more phosphorylatable residues. Moreover, phosphorylation of the activation segment is necessary for the expression of maximal enzyme activity in nearly all protein kinases. In contrast, ErbB1/2/4 of the EGFR family exhibit maximal activity in the absence of activation segment phosphorylation. The initial part (DFG) of the activation segment occurs spatially near the conserved catalytic loop HRD sequence and the amino-terminus of the αC-helix. This helix, which occurs within the small lobe, nevertheless occupies a strategically important position between both lobes. The activation segment of protein kinases has an extended and open structure in the active form of all protein kinases (Fig. A) and a closed structure in most dormant kinases (Fig. 1C/E) [2]. The initial two residues of the activation segment occur in different conformations. The DFG-D side chain of operational protein kinases faces the ATP-binding site and it binds $Mg^{2+}(1)$. This configuration is called the "DFG-$D_{in}$" conformation (Fig. 1A/C). In the dormant activation segment configuration that is observed in many protein kinase structures, the DFG-D points away from the ATP-binding site. This structure is called the "DFG-$D_{out}$" conformation (Fig. 1/E). It is the ability of DFG-*D* to bind (DFG-$D_{in}$) or not bind (DFG-$D_{out}$) $Mg^{2+}(1)$ within the active site that is important.

Modi and Dunbrack performed an all-inclusive analysis of the interaction of drugs with active and dormant conformations of protein kinases based upon the organization of the activation loop, which begins with the DFG sequence [26,27]. As noted, this signature is observed in two major classes of conformations: DFG-$D_{in}$ and DFG-$D_{out}$. In the first case the phenylalanine residue contacts the αC-helix of the N-terminal lobe and in the second case phenylalanine occupies a portion of the ATP site thereby generating an αC-helix pocket. These investigators found a clustering of protein kinase conformations that relied on the location of the phenylalanine side chain (DFG-$D_{in}$, DFG-$D_{out}$, and DFG-$D_{intermediate}$)

**Table 2**
Important residues in selected human protein kinases.

| | FGFR1 | FGFR2 | MET | VEGFR2 |
|---|---|---|---|---|
| Number of residues | 822 | 821 | 1390 | 1356 |
| Signal peptide | 1–21 | 1–21 | 1–24 | 1–19 |
| Extracellular segment | 22–376 | 22–377 | 25–932 | 20–764 |
| Transmembrane segment | 377–397 | 378–398 | 933–955 | 765–785 |
| Intracellular portion | 398–822 | 399–821 | 956–1390 | 786–1356 |
| Protein kinase domain | 478–767 | 481–770 | 1078–1345 | 834–1162 |
| Glycine-rich loop | $^{485}$GEGCFG$^{490}$ | $^{488}$GEGCFG$^{493}$ | $^{1085}$GRGHFG$^{1090}$ | $^{841}$GRGAFG$^{846}$ |
| The β3-*K* of K/*E*/D/D | K514 | K517 | K1110 | K868 |
| αC-*E* of K/*E*/D/D | E531 | E534 | E1127 | E885 |
| Hinge-linker residues | $^{562}$EYASKGN$^{568}$ | $^{565}$EYASKGN$^{571}$ | $^{1158}$PYMKHDG$^{1164}$ | $^{917}$EFCKFGN$^{923}$ |
| Gatekeeper residue | V561 | V564 | L1157 | V916 |
| Catalytic HR*D* residue, the first *D* of K/E/*D*/D | D623 | D626 | D1204 | D1028 |
| Catalytic loop | $^{621}$HRDLAARN$^{628}$ | $^{624}$HRDLAARN$^{631}$ | $^{1202}$HRDLAARN$^{1209}$ | $^{1026}$HRDLAARN$^{1033}$ |
| AS[a] *D*FG, the second *D* of K/E/D/*D* | D641 | D644 | D1222 | D1046 |
| AS[a] tyrosine phosphorylation site | Y653/654 | Y656/7 | Y1230, Y1234/5 | Y1054/Y1059 |
| End of the AS[a] | $^{668}$APE$^{670}$ | $^{671}$APE$^{673}$ | $^{1251}$ALE$^{1253}$ | $^{1073}$APE$^{1075}$ |
| Molecular weight (kDa) | 91.9 | 92.0 | 155.5 | 151 |
| UniProtKB ID | P11362 | P21802 | P08581 | P35968 |

[a] AS, activation segment.

and the backbone dihedral angles of the xDF sequence (x is the residue before the DFG signature). They identified eight distinctive conformations and labeled them based on the Ramachandran regions (A, alpha; B, beta; L, left) of the xDF motif and the configuration (χ1) of the phenylalanine rotamer (minus, plus, trans). Their clusters divide the DFG-$D_{in}$ configuration into six groups including BLAminus, which contains active structures, and two common inactive forms, ABAminus and BLBplus. $DFG_{out}$ structures are found mainly in the BBAminus

**Table 3**
Blue Ridge Institute for Medical Research (BRIMR), Modi-Dunbrack Fox Chase Cancer Center (FCCC), and Kinase Ligand Interaction and Fingerprint and Structure (KLIFS) inhibitor data base comparisons.

| Ligand/Drug-enzyme | PDB ID | BRIMR type[a] | FCCC type[b,c] | FCCC: Dihedral angles & DFG-D[c] | KLIFS pockets[d] |
|---|---|---|---|---|---|
| ADP-AurkA | 4dee | I | I | BLAminus & DFG-$D_{in}$ | F, FP-II |
| *BRIMR type I inhibitors* | | | | | |
| Bosutinib-Src | 4mxo | I | I | BLAminus & DFG-$D_{in}$ | F,G, BP-I-A/B |
| Dasatinib-Abl | 2gqg | I | I, I½b | BLAminus & DFG-$D_{in}$ | F, G, B, BP-I-A/B |
| Erlotinib-EGFR | 1m17 | I | I | BLAminus & DFG-$D_{in}$ | F, G, B, BP-I-A/B |
| Gefitinib-EGFR | 2ity | I | I | BLAminus & DFG-Din | F,G, BP-I-A/B |
| Palbociclib-CDK6 | 2euf | I | I | BLAminus & DFG-$D_{in}$ | F |
| Pralsetinib-RET | 7ju5 | I | I | BLAminus & DFG-$D_{in}$ | F, FP-II |
| R406 (fostamatinib) | 3fqs | I | I | BLAminus & DFG-$D_{in}$ | F |
| Selpercatinib-RET | 7ju6 | I | I½f | BLAminus & DFG-$D_{in}$ | F, FP-II |
| Vandetanib-RET | 2ivu | I | I | BLAminus & DFG-$D_{in}$ | F,G, BP-I-A/B |
| *BRIMR type I½A inhibitors* | | | | | |
| Dabrafenib-B-Raf | 5csw | I½A | I½b | BLBminus & DFG-$D_{in}$ | F, G, B, FP-II, BP-I-A/B, BP-II-in, BP-II-A-in |
| Erdafitinib-FGFR1 | 5ew8 | I½A | I½b | BLAplus & DFG-$D_{in}$ | F, G, B, FP-I, BP-I-A/B |
| Infigratinib-FGFR1 | 3tt0 | I½A | I½b | BLAplus & DFG-$D_{in}$ | F, G, B, BP-I-A/B |
| Lapatinib-EGFR | 1xkk | I½A | I½b | BLAplus & DFG-$D_{in}$ | F, G, B, BP-I-A/B, BP-II-in, BP-II-A-in |
| Lenvatinib-VEGFR2 | 3wzd | I½A | I | BLBplus & DFG-$D_{in}$ | F, G, B, BP-I-B, BP-II-in |
| Vemurafenic-B-Raf | 3og7 | I½A | I½b | BLAplus & DFG-$D_{in}$ | F, G, B, FP-I, BP-I-A/B, BP-II-in, BP-II-A-in |
| *BRIMR type I½B inhibitors* | | | | | |
| Abemeciclib-CDK6 | 5l2s | I½B | I | BLBplus & DFG-$D_{in}$ | F, FP-II |
| Alectinib-ALK | 3aox | I½B | I | ABAminus & DFG-$D_{in}$ | F, BP-I-B |
| Brigatinib-ALK | 6mx8 | I½B | I | ABAminus & DFG-$D_{in}$ | F, FP-I |
| Ceritinib-ALK | 4mkc | I½B | I | ABAminus & DFG-$D_{in}$ | F, FP-I |
| Crizotinib-ALK | 2xp2 | I½B | I | ABAminus & DFG-$D_{in}$ | F, FP-I |
| Crizotinib-MET | 2wgj | I½B | I | BLBplus & DFG-$D_{in}$ | F, FP-I |
| Crizotinib-ROS1 | 3zbf | I½B | I | ABAminus & DFG-$D_{in}$ | F, FP-I |
| Entrectinib-TRKA | 5kvt | I½B | I | ABAminus & DFG-$D_{in}$ | F, FP-I |
| Erlotinib-EGFR | 4hjo | I½B | I | BLBtrans & DFG-$D_{in}$ | F, G, BP-I-A/B |
| Lorlatinib-ALK | 4cli | I½B | I | ABAminus & DFG-$D_{in}$ | F, FP-I |
| Palbociclib-CDK6 | 5l2i | I½B | I | BLBplus & DFG-$D_{in}$ | F |
| Ribociclib-CDK6 | 5l2t | I½B | I | BLBplus & DFG-$D_{in}$ | F, G, FP-I |
| Tepotinib-MET | 4r1v | I½B | I | BLBplus & DFG-$D_{in}$ | F, FP-I |
| Tofacitinib-JAK1 | 3eyg | I½B | I | ABAminus & DFG-$D_{in}$ | F, FP-I/II |
| Tofacitinib-JAK3 | 3lxk | I½B | I | ABAminus & DFG-$D_{in}$ | F, FP-I/II |
| *BRIMR type IIA inhibitors* | | | | | |
| Axitinib-VEGFR2 | 4ag8 | IIA | I | BBAminus & DFG-$D_{out}$ | F, G, B, BP-I-B, BP-II-out |
| Imatinib-Abl[e] | 1iep | IIA | II | BBAminus & DFG-$D_{out}$ | F, G, B, BP-I-A/B, BP-II-out, BP-IV |
| Imatinib-Kit | 1t46 | IIA | II | BBAminus & DFG-$D_{out}$ | F, G, B, BP-I-A/B, BP-II-out, BP-IV |
| Nilotinib-Abl | 3cs9 | IIA | II | BBAminus & DFG-$D_{out}$ | F, G, B, BP-I-A/B, BP-II-out, BP-III, BP-V |
| Pexidartinib-CSF1R | 4r7h | IIA | II | BBAminus & DFG-$D_{out}$ | F, G, B, BP-I-B, BP-II-out, BP-V |
| Ponatinib-Abl[e] | 3oxz | IIA | II | BBAminus & DFG-$D_{out}$ | F, G, B, BP-I-A/B, BP-II-out, BP-III, BP-IV |
| Ripretinib-Kit | 6mob | IIA | II | BBAminus & DFG-$D_{out}$ | F, G, B, BP-I-A/B, BP-II-out, BP-III |
| Sorafenib-B-Raf | 1uwh | IIA | II | BBAminus & DFG-$D_{out}$ | F, G, B, BP-I-B, BP-II-out |
| Sorafenib-CDK8 | 3rgf | IIA | II | BBAminus & DFG-$D_{out}$ | F, G, B, BP-I-B, BP-II-out, BP-III |
| Sorafenib-VEGFR2 | 4asd | IIA | II | BBAminus & DFG-$D_{out}$ | F, G, B, BP-I-B, BP-II-out, BP-III |
| Tivozantinib-VEGFR2 | 4ase | IIA | II | BBAminus & DFG-$D_{out}$ | F, G, B, BP-I-B, BP-II-out |
| *BRIMR type IIB inhibitors* | | | | | |
| Bosutinib-Abl | 3ue4 | IIB | I | Unassigned & DFG-$D_{out}$ | F, G, BP-II-A/B |
| Gilteritinib-FLT3 | 6jqr | IIB | I | Unssigned & DFG-$D_{out}$ | F |
| Nintedanib-VEGFR2 | 3c7q | IIB | I | Unassigned & DFG-$D_{out}$ | F, G, BP-I-B |
| Sunitinib-Kit | 3g0e | IIB | I | Unassigned & DFG-$D_{out}$ | F |
| Sunitinib-VEGFR2 | 4agd | IIB | I | BBAminus & DFG-$D_{out}$ | F, BP-I-B |
| *BRIMR type III inhibitors* | | | | | |
| Cobimetinib-MEK1 | 4an2 | III | III, I | BLBplus & DFG-$D_{in}$ | G, B, BP-II-in |
| Selumetinib-MEK1 | 4u7z | III | III, I | BLBplus & DFG-$D_{in}$ | G, B, BP-II-in |
| *BRIMR type VI inhibitors* | | | | | |
| Afatinib-EGFR | 4g5j | VI | I | BLAminus & DFG-$D_{in}$; allosteric | F, G, BP-I-A/B |
| Dacomitinib-EGFR | 4i24 | VI | I | BLBtrans & DFG-$D_{in}$ | F, G, BP-I-B |
| Ibrutinib-BTK | 5p9j | VI | I½b | BLBplus & DFG-$D_{in}$ | F, G, B, BP-I-B |
| Neratinib-EGFR | 2jiv | VI | I½b | BLBplus & DFG-$D_{in}$ | F, G, B, BP-I-A/B |
| Osimertinib-EGFR | 6jxt | VI | I | BLBtrans & DFG-$D_{in}$ | F |
| Zanubrutinib-BTK | 6j6m | VI | I½b | BLBplus & DFG-$D_{in}$ | F, G, B, BP-I-B |

[a] Ref. [31]
[b] b, back; f, front
[c] From Ref. [27] and http://dunbrack3.fccc.edu/kincore/
[d] klifs.net
[e] Mouse enzyme

conformation. The inactive conformations possess features that prevent their binding to ATP, magnesium, and/or their protein substrates. These investigators produced a valuable and noncommercial web site (http://dunbrack3.fccc.edu/kincore/) that allows one to determine whether the protein kinase conformations corresponds to an active enzyme (DFG-$D_{in}$, BLAminus) or to a dormant enzyme (DFG-$D_{in}$, BLBplus, DFG-$D_{in}$, ABAminus, DFG-$D_{out}$, BBAminus). We used this web site to decide whether the conformation of the various protein kinases of the drug-enzyme complexes that we are considering are active (DFG-$D_{in}$, BLAminus) or dormant (otherwise). Table 3 provides a comparison of the BRIMR and the Modi-Dunbrack schemes. See Refs. [2,26,27] for more information about these and related DFG activation segment arrangements.

### 2.2. Protein kinase hydrophobic skeletons

Kornev et al. studied the three-dimensional structures of active and inactive configurations of about two dozen protein kinases to identify structurally and functionally important residues [28,29]. Their analyses revealed a combination of four amino acids that make up a regulatory spine or R-spine and eight amino acids along with the adenine base of ATP that make up a catalytic spine or C-spine. These residues occur in both the small and large lobes. The regulatory and catalytic spines generate a stable, but flexible, catalytically active ensemble. The R-spine helps to position the protein substrate and the C-spine helps to position ATP for catalysis. The R-spine contains components from both the αC-helix and activation segment, whose structures are important in determining active and dormant enzyme states. The precise alignment and positioning of both spines are necessary, but not sufficient, for the creation of a catalytically competent protein kinase.

The R-spine contains the first residue of the β4-strand along with an amino acid exactly four residues amino-terminal to the conserved αC-helix glutamate, which are within the amino-terminal lobe [28]. The R-spine also contains the DFG-phenylalanine of the activation segment and the HRD-histidine of the catalytic loop, both within the large lobe. The HRD-histidine N–H backbone forms a hydrogen bond with the side chain of a conserved aspartate within the hydrophobic αF-helix. From the base to the apex, Meharena et al. labeled the R-spine residues as RS0, RS1, RS2, RS3, and RS4 [30]. We later labeled the C-spine residues from the base to the apex as residues CS1–8 (Fig. 1) [31]. Note that the C- and R-spines of active protein kinases are linear (Fig. 1B). In protein kinases with the $\alpha C_{out}$ structure, RS3 is displaced toward the right as protein kinases are usually depicted. In enzymes with the DFG-$D_{out}$ structure, RS2 (the DFG-D residue) is displaced toward the left and the R-spine is broken (Fig. 1F). The R-spine, C-spine, and shell residues of four protein kinases considered in this review are listed in Table 4.

The protein kinase spine and shell residues play a key role in the structure and activity of these enzymes; it is not possible to overemphasize their importance in the functioning of this enzyme superfamily as well as their interactions with small molecule protein kinase blockers. For a review of the properties of the spine and shell residues and their interactions with small molecule inhibitors of selected members of the protein kinase superfamily, see the following reviews: Refs. [32–34] for the EGFR family of protein-tyrosine kinases, Refs. [35–37] for the ALK pleotrophin and midkine receptor protein-tyrosine kinase, Ref. [38] for the fibroblast growth factor receptor family of protein-tyrosine kinases, Ref. [39] for the PDGFRα/β protein-tyrosine kinases, Ref. [40] for the Kit stem cell receptor protein-tyrosine kinase, Ref. [41] for the VEGFR1/2/3 protein-tyrosine kinases, Ref. [42] for the RET glial-cell derived receptor protein-tyrosine kinase, Ref. [43] for the Flt3 receptor protein-tyrosine kinase; Ref. [44] for the ROS1 orphan receptor protein-tyrosine kinase, Refs. [45,46] for the Src nonreceptor protein-tyrosine kinase, Ref. [47] for the Bruton nonreceptor protein-tyrosine kinase, Ref. [48] for the Janus nonreceptor protein-tyrosine kinase, Refs. [49,50] for the MEK1/2 dual specificity protein kinases, Refs. [51,52] for the RAF protein-serine/threonine kinase, Refs. [53,54] for the ERK1/2 protein-serine/threonine kinases, and Refs. [19,55] for the cyclin-dependent protein-serine/threonine kinase family.

**Table 4**
Spine and shell residues of human FGFR1, FGFR2, MET and VEGFR2.

| | Symbol | KLIFS No.[a] | FGFR1 | FGFR2 | MET | VEGFR2 |
|---|---|---|---|---|---|---|
| *Regulatory spine* | | | | | | |
| β4-strand (N-lobe) | RS4 | 38 | L547 | L550 | L1142 | L901 |
| C-helix (N-lobe) | RS3 | 28 | M535 | M538 | M1131 | L889 |
| Activation loop DFG-F (C-lobe) | RS2 | 82 | F642 | F654 | F1223 | F1047 |
| Catalytic loop HRD-H (C-lobe) | RS1 | 68 | H621 | H624 | H1202 | H1026 |
| F-helix (C-lobe) | RS0 | None | D682 | D685 | D1265 | D1087 |
| *Shell* | | | | | | |
| Two residues upstream from the gatekeeper | Sh3 | 43 | V559 | V562 | V1155 | V914 |
| Gatekeeper, end of β5-strand | Sh2 | 45 | V561 | V564 | L1157 | V916 |
| αC-β4 loop | Sh1 | 36 | I545 | I548 | L1140 | V899 |
| *Catalytic spine* | | | | | | |
| β3-AxK motif (N-lobe) | CS8 | 15 | A512 | A515 | A1108 | A666 |
| β2-strand (N-lobe) | CS7 | 11 | V492 | V495 | V1092 | V848 |
| β7-strand (C-lobe) | CS6 | 77 | L630 | L733 | M1211 | L1035 |
| β7-strand (C-lobe) | CS5 | 78 | V631 | V634 | L1212 | L1036 |
| β7-strand (C-lobe) | CS4 | 76 | V629 | V632 | C1210 | I1034 |
| D-helix (C-lobe) | CS3 | 53 | L569 | L572 | L1165 | L924 |
| F-helix (C-lobe) | CS2 | None | L689 | L692 | L1272 | L1094 |
| F-helix (C-lobe) | CS1 | None | I693 | I696 | L1276 | I1098 |

[a] From Refs. [64–66].

The C-spines of protein kinases consist of two residues from the amino-terminal lobe and six residues from the carboxyterminal lobe. The adenine base of ATP combines these two parts of the C-spine and this process facilitates the merging of the two lobes of the enzyme and readies the enzyme for catalysis [29]. The two amino-terminal lobe residues that bind to the adenine base of ATP include the conserved β2-strand valine (CS7) after the glycine-rich loop and the conserved β3-strand alanine (CS8) of the AxK motif. A hydrophobic residue from the middle of the large lobe β7-strand (CS6) interacts with the adenine base of ATP. Furthermore, CS4 and CS5 interact with CS3 at the beginning of the αD-helix. Additionally, CS3 makes hydrophobic contact with (i) the adjacent CS4 and (ii) CS1 within the αF-helix below it. Both the R- and C- spines are supported by the hydrophobic αF-helix below them; the αF-helix serves as a major support for the stabilization of the entire protein kinase domain and it contains CS1, CS2, and RS0 (Fig. 1). The protein kinase hinge and linker residues connect the amino-terminal and carboxyterminal lobes of protein kinases and the 6-amino group of ATP hydrogen bonds with the backbone carbonyl group of the first hinge residue. Furthermore, the *N*1 of the adenine base of ATP hydrogen bonds with the backbone N–H group of the third hinge residue (Fig. 1A). Nearly all ATP small-molecule steady-state competitive protein kinases inhibitors hydrogen bond with backbone hinge residues, usually with that of the third hinge residue [31].

Based upon the findings of site-directed mutagenesis studies, Meharena et al. identified three residues in murine protein kinase A that strengthen the regulatory spine, which they labeled as shell residues (Sh1, Sh2, and Sh3) [30]. While their Sh1 mutant (V104G) had 5% of the catalytic activity of the wild type enzyme, their Sh2/Sh3 double mutant (M120G/M118G) was kinase dead. These results demonstrated that the shell residues support PKA activity. We infer that shell residues play a

similar stabilizing role for all protein kinases. The Sh1 residue is found within the segment connecting the αC-helix and the β4-strand, the so-called back loop. The Sh2 residue (the gatekeeper) occurs at the end of the β5-strand immediately before the hinge region and the Sh3 residue is found within the β5-strand two residues upstream from the Sh2 residue (Fig. 1D).

The term gatekeeper indicates the role that this residue plays in controlling access to the hydrophobic pocket adjoining the adenine binding pocket [56,57], a pocket that often interacts with structural components of numerous small molecule protein kinase inhibitors. Based upon the findings of Meharena et al. [30], only three of the 14 amino acids near RS3 and RS4 in protein kinase A are conserved. It is important to note that many small molecule therapeutic steady-state ATP-competitive protein kinase antagonists interact with the C-spine (CS6/7/8), the R-spine (RS2/3), and shell (Sh1 and Sh2) residues. Ung et al. reported that about three-fourths of protein kinases have a relatively large gatekeeper residue (e.g., Met, Leu, Phe) while about one-fourth have smaller gatekeeper residues (e.g., Thr, Val) [58]. Also of importance in the consideration of long-term drug efficacy, the gatekeeper residue is one of the more common sites of drug-resistant mutations [3,59].

## 3. Protein kinase-inhibitor classification and inhibitor-binding pockets

Based upon previous studies [57,60–62], we divided the small molecule protein kinase antagonists into seven main classes including reversible (Groups I, I½, II, III, IV, and V) and targeted covalent irreversible inhibitors (VI) as described in Table 5. We split the type I½ and type II inhibitors into A and B subtypes [31]. Subtype A drugs are those that extend past the gatekeeper residue into the back cleft. In comparison, subtype B drugs are those that do not extend into the back cleft. The potential significance of this difference, based on incomplete data, is that subtype A inhibitors bind to their protein target with longer residence times when compared with subtype B inhibitors [31]. For example, sorafenib is a type IIA VEGFR inhibitor and sunitinib is a type IIB VEGFR antagonist, both of which are FDA-approved for the treatment of renal cell carcinomas. The type IIA inhibitor has a residence time greater than 64 min while the type IIB antagonist has a residence time less than 2.9 min [31].

We followed the results of Liao [63], van Linden et al. [64], Kooistra et al. [65], and Kanev et al. [66] in defining and differentiating drug-binding pockets. A broad overview describing the location of the pockets and subpockets is depicted in Fig. 2 and the position of important residues lining these pockets is described in Table 6. The region between the protein kinase N-terminal and C-terminal lobes is divided into a front pocket or front cleft, a gate area, and a back cleft. The back pocket (HPII, hydrophobic pocket II) includes the gate area and the adjacent back cleft. The front cleft includes the glycine-rich loop (GRL), the adenine-binding pocket (AP), the hinge residues, the linker residues that connect the hinge residues to the αD-helix in the large lobe, and the catalytic loop $(HRD(x)_4N)$.

Type I inhibitors normally bind within the front cleft. The gate area includes residues from both the N-terminal and C-terminal lobes. The gate area includes the last three residues of the β3-strand and the first two residues of the β3-αC loop. It also includes the residue immediately before the activation segment (the x of xDFG) together with the first four residues of the activation segment. The back cleft contains the middle portion of the αC-helix, the β4-strand along with the last two residues of the β5-strand. The back cleft also contains the first two and fifth residues of the large lobe αE-helix and the two residues preceding the catalytic loop HRD (Fig. 2C). Many type I½ inhibitors occupy both the front cleft and a fragment of the back cleft. One of the overall goals in the creation of small molecule protein kinase antagonists is to maximize selectivity to reduce off-target side effects [61]; this strategy can be facilitated by comparing drug interactions with target and nontarget enzymes [67–69]. Designing drug fragments that interact with residues lining the various pockets within the cleft plays a strategic role in protein kinase inhibitor development with the goal of maximizing drug affinity.

van Linden et al. and Kanev et al. described ligand and drug binding to more than 5200 human and mouse protein kinase domains [64,66]. Their KLIFS (kinase–ligand interaction fingerprint and structure) catalog includes an alignment of 85 ligand binding-site residues that are found in both the amino-terminal and carboxyterminal lobes; their guide facilitates the description of ligands and drugs depending upon their binding properties. These data assist in the recognition of common and unique drug-enzyme interactions. These authors formulated a standard amino acid residue numbering scheme that facilitates the comparison of different protein kinase targets. Table 6 describes the relationship of the KLIFS database nomenclature and the R-spine, C-spine, and shell amino acid residue numbering system and Fig. 3 depicts the location of the KLIFS residues within the protein kinase domain. Furthermore, these authors launched a valuable noncommercial and searchable web site that is regularly updated that provides complete data on the interaction of protein kinases with ligands and drugs (klifs.net).

Additionally, Carles et al. produced a comprehensive tally of protein kinase antagonists that have been approved or that are in clinical trials [6]. They created a noncommercial and searchable web site that is regularly updated that includes the structure of the various drugs, their protein kinase targets, physical properties, therapeutic indications, the year of first approval (if applicable), and their trade name (http://www.icoa.fr/pkidb/). Similarly, the Blue Ridge Institute for Medical Research (BRIMR) maintains a web site that lists the FDA-approved protein kinase antagonists and depicts their (i) structures, (ii) number of hydrogen bond donors/acceptors, (iii) calculated Log of the partition coefficients and distribution coefficients, (iv) number of rings and rotatable bonds, (v) year of initial approval, (vi) primary protein kinase targets, (vii) and clinical indications. The site also provides a link to the corresponding FDA labels. This web site, which is found at www.brimr.org/PKI/PKIs.htm, is updated following FDA-approval of new protein kinase inhibitors.

**Table 5**
Classification of small molecule protein kinase inhibitors[a].

| Inhibitor type | Properties |
|---|---|
| I | Binds in and around the ATP-binding pocket of an active enzyme |
| I½ A/B | Binds in and around the ATP-binding pocket of an inactive DFG-$D_{in}$ enzyme |
| I½ A | Extends into the back cleft |
| I½ B | Does not extend into the back cleft |
| II A/B | Bind in and around the ATP-binding site of an inactive DFG-$D_{out}$ enzyme |
| II A | Extends into the back cleft |
| II B | Does not extend into the back cleft |
| III | Allosteric inhibitor bound next to the ATP-binding site |
| IV | Allosteric inhibitor bound away from the ATP-binding site |
| V | Bivalent inhibitor spanning two kinase domain regions |
| VI | Covalent inhibitor |

[a] Adapted from Ref. [31].

## 4. Drug-enzyme interactions: infigratinib, tepotinib, tivozanib

Infigratinib is an anilino-pyrimidine derivative (Fig. 4A) [70] that is FDA-approved for the treatment of cholangiocarcinomas bearing FGFR2 fusion proteins [71]. We lack the X-ray crystal structure of infigratinib bound to FGFR2, but we have the structure of the drug bound to the related FGFR1 [70]. It shows that the pyrimidine nitrogen binds to the N–H group and the anilino N–H group binds to the backbone carbonyl group of the third hinge residue (A564) (Fig. 5A). The piperazine N–H binds to the side chain of E571 and a methoxy oxygen hydrogen bonds with the N–H group of DFG-D641. The drug makes hydrophobic contact

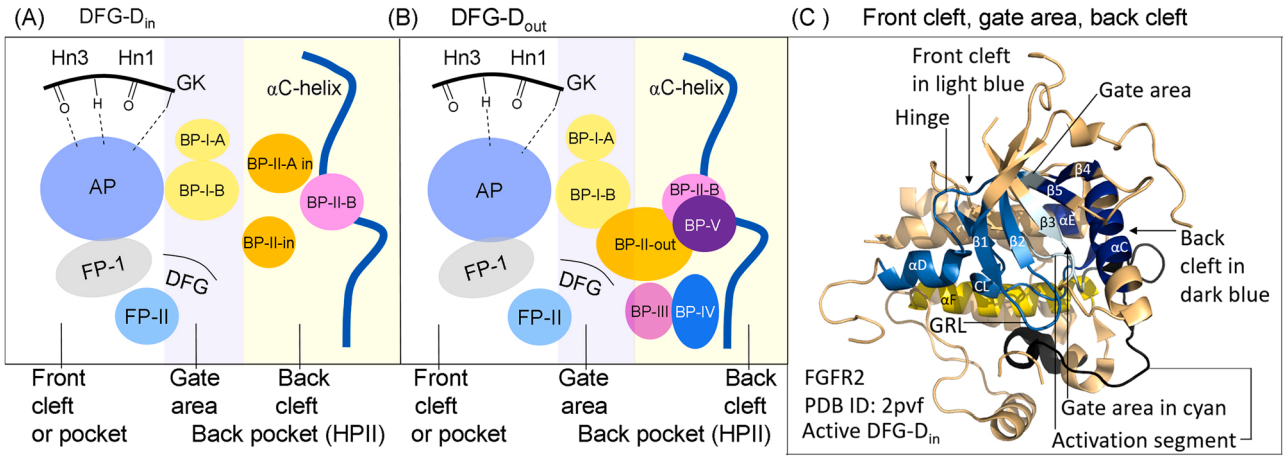


**Fig. 2.** (A) Location of the protein kinase domain drug-binding pockets in the DFG-$D_{in}$ enzyme form. (B) Locaion of the drug-binding pockets in the DFG-$D_{out}$ enzyme form. (C) Location of the protein kinase front cleft, gate area, and back cleft. AP, adenine pocket; BP, back pocket; FP, front pocket; GRL, glycine-rich loop; Hn, hinge; HPII, hydrophobic pocket II; GK, gatekeeper.
Adapted from Refs. [63–66].

**Table 6**
Location of important residues within the front cleft, gate area, and back cleft.

| Description | Location | KLIFS residue no.[a] |
|---|---|---|
| GxGxΦG | Front cleft | 4–9 |
| β2-strand V (CS7) | Front cleft | 11 |
| β3-strand A (CS8) | Front cleft | 15 |
| HRD with DFG-$D_{in}$ | Front cleft | 68–70 |
| $HRD(x)_4N$-N | Front cleft | 75 |
| β7-strand CS6 | Front cleft | 77 |
| β3-strand K | Gate area | 17 |
| αC-β4 penultimate back loop residue | Gate area | 36 |
| Gatekeeper | Gate area | 45 |
| The x of xDFG | Gate area | 80 |
| DFG | Gate area | 81–83 |
| αC-helix E | Back cleft | 24 |
| RS3 | Back cleft | 28 |
| HRD with DFG-$D_{out}$ | Back cleft | 68–70 |

[a] Refs. [64–66].

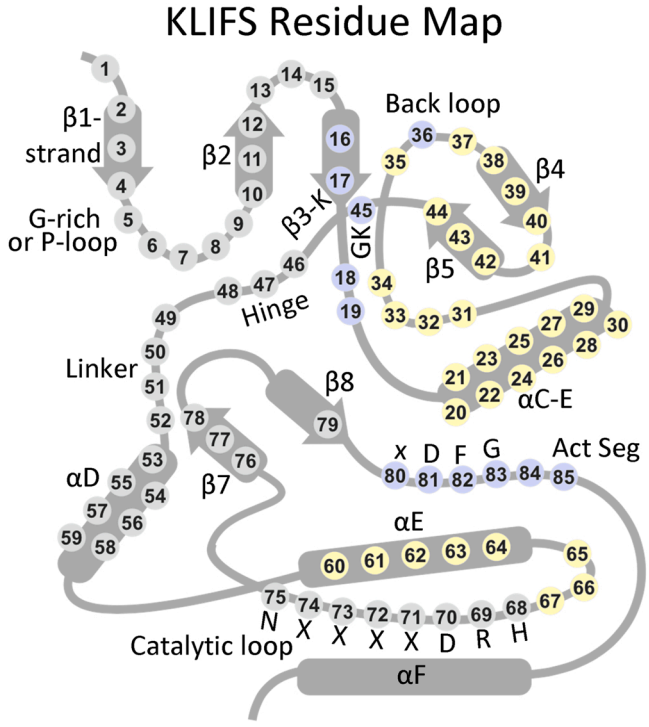


**Fig. 3.** The location of the KLIFS residues within a generic protein kinase domain. Act Seg, activation segment. Residues in gray circles are found in the front cleft; blue circles, gate area; yellow circles, back cleft.

with the three spine residues (CS6/7/8), three shell residues (Sh1/2/3), and L484 (the KLIFS-3 residue) (Table 7). The agent also makes hydrophobic contact with V513 of the β3-strand, AxK-K514, αC-E531 and E562, Y563, and A564 of the hinge, and G567 of the linker. The compound makes additional hydrophobic contact with A640 (the x of xDFG), DFG-D641, and DFG-F642. These interactions are included in the supplementary material. The drug binds to the front pocket, gate area, and back pocket as well as subpockets BP-I-A/B of an inactive DFG-$D_{in}$ enzyme and is classified as a type I½A inhibitor [31]. Modi and Dunbrack indicate that this enzyme occurs within the BLAplus cluster and label it a type 1.5 back inhibitor [28]. See Ref. [71] for information on the clinical trials that led to the approval of infigratinib.

Tepotinib is a phenylmethyl-pyrimidine derivative (Fig. 4B) that is FDA-approved for the treatment of adult patients with metastatic non-small cell lung cancer (NSCLC) harboring mesenchymal epithelial transition (MET) exon 14 skipping alterations [72]. MET is a receptor protein-tyrosine kinase whose activating ligand is hepatocyte growth factor/scatter factor (HGF/SF) [37]. The term 'MET' originally referred to the methyl group in the carcinogen (*N*-methyl-*N*′-nitro-*N*-nitrosoguanidine) used in generating the fusion protein in a human osteogenic sarcoma cell line [37]. In addition to its role in promoting cell division and survival, MET also plays a role in the metastasis of cancer cells. MET may be thought of as an abbreviation for 'metastasis' or an acronym for 'mesenchymal-epithelial transition' factor [37]. The X-ray crystal structure of tepotinib bound to MET demonstrates that the pyrimidine nitrogen hydrogen bonds with the N–H group of M1160 (the third hinge residue) and the oxygen attached to the pyridazine hydrogen bonds to the N–H group of DFG-D1222 (Fig. 5B). The drug makes hydrophobic contact with three spine residues (CS6/7/8), two shell residues (Sh2/3), and I1084 (the KLIFS-3 residue). It also makes hydrophobic contact with G1085 of the glycine-rich loop, and $^{1158}$PYMKHGD$^{1164}$ of the hinge-linker segment, two catalytic loop residues (R1208, N1209), the x of xDFG (A1221), and DFG-D1222. The enzyme assumes an inactive DFG-$D_{in}$ and αC$_{out}$ conformation (Fig. 1C) and the drug occupies the front pocket and FP-I and does not extend into the gate area or back pocket; it is therefore classified as a type I½B inhibitor [31]. Modi and Dunbrack consider this to be a type I inhibitor with a BLBplus

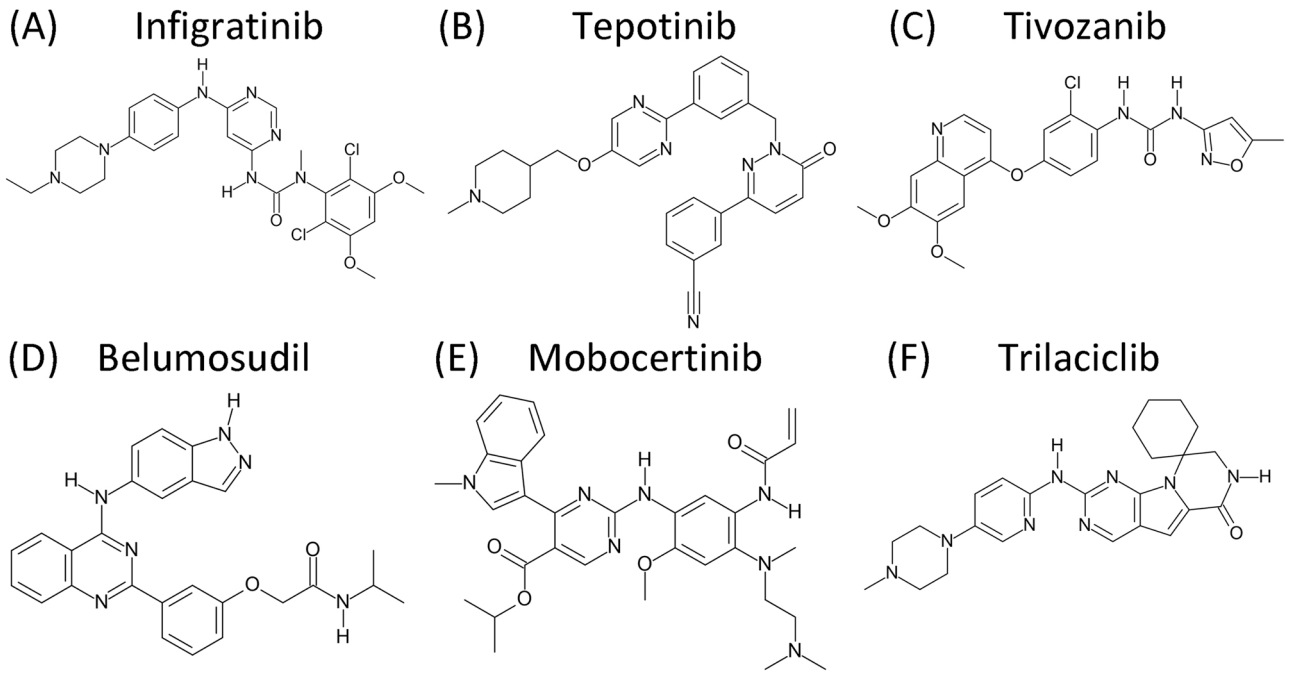


**Fig. 4.** (A-F). Chemical structures of selected protein kinase inhibitors.

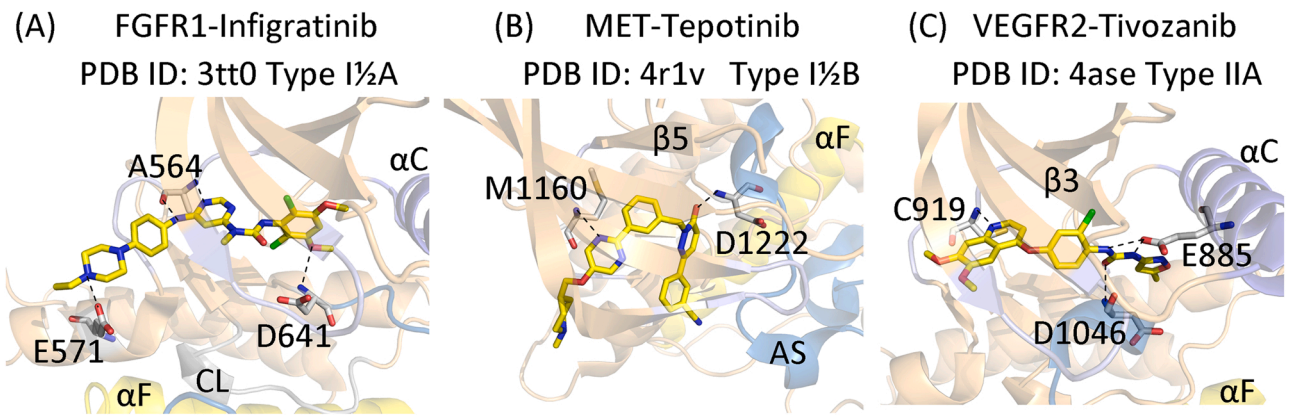


**Fig. 5.** (A) Infigratinib-FGFR1. (B) Tepotinib-MET. (C) Tivozanib-VEGFR2. The drug carbon atoms are colored yellow and the dashed lines represent polar bonds. AS, activation segment; CL, catalytic loop.

structure [28]. See Refs. [72,73] for a summary of the clinical trials that led to its approval.

Tivozanib is a quinoline-urea derivative (Fig. 4C) that is FDA-approved for the third-line treatment of renal cell carcinoma [74,75]. This compound is a potent VEGFR2 inhibitor. The X-ray crystal structure of tivozanib bound to VEGFR2 shows that the quinazoline nitrogen hydrogen bonds with the N–H group of C919 (the third hinge residue), the N–H groups of urea bind to αC-E885, and the urea carbonyl group hydrogen bonds to the N–H group of DFG-D1046 (Fig. 5C). Type IIA inhibitors characteristically form a hydrogen bond with a hinge residue, the αC-E sidechain, and the DFG-$D_{out}$ N–H group as observed here [10]. The drug makes hydrophobic contact with five spine residues (RS2/3, CS6/7/8) and L840 (the KLIFS-3 residue) (Table 7). Tivozanib also makes hydrophobic contact with G842 of the glycine-rich loop, AxK-K868, αC-E885, three hinge residues (E917, F918, L919), two linker residues (K920, G922), C1045 (the x of xDFG), and DFG-D1046. The conformation has $\alpha C_{in}$ and DFG-$D_{out}$ (Fig. 1E) and the drug occupies the front cleft, gate area, back cleft, BP-I-B and BP-II-out, which corresponds to a type IIA inhibitor [31]. In agreement, Modi and Dunbrack consider this to be a type II inhibitor with a BBAminus structure. See Ref. [75] for a summary of the clinical trials that led to its approval.

## 5. Newly approved protein kinase antagonists without drug-enzyme structures: belumosudil, mobocertinib, trilaciclib

Belumosudil is an indazole-quinazoline derivative (Fig. 4D) that is FDA-approved for the third-line treatment of chronic graft vs. host disease [76–78]. This drug inhibits the ROCK2 protein-serine/threonine kinases that are downstream targets of the small RhoA, RhoB, and RhoC GTPases that are involved in diverse cellular activities including cell adhesion and motility, stress fiber and focal adhesion formation, actin cytoskeletal reorganization, remodeling of the extracellular matrix, and the control of profibrotic pathways. ROCK2 refers to Rho-associated coiled-coil containing protein kinase 2. The *ROCK2* gene protein contains 1388 amino acids with a molecular weight of 160.9 kDa. Chronic graft vs. host disease is an immune-mediated inflammatory and fibrotic disease. It is a primary cause of morbidity, mortality, and impaired quality of life after an allogeneic hematopoietic cell transplant. The first line treatment of this malady includes administration of corticosteroids alone or in combination with sirolimus [79].

**Table 7**
Drug-enzyme hydrophobic (Φ) and hydrogen-bond (A, D) interactions based upon their common KLIFS residue numbers[a,b,c,d,e].

| | PDB ID | RS1 | RS2 | RS3 | RS4 | Sh1 | Sh2 | Sh3 | CS5 | CS6 | CS7 | CS8 | KLIFS-3[d] | KLIFS pockets[a] |
|---|---|---|---|---|---|---|---|---|---|---|---|---|---|---|
| KLIFS no. → | | 68 | 82 | 28 | 38 | 36 | 45 | 43 | 76 | 77 | 11 | 15 | 3 | |
| Drug-enzyme ↓ | | | | | | | | | | | | | | |
| *Type I inhibitors* | | | | | | | | | | | | | | |
| Bosutinib-Src | 4mxo | | | Φ | | Φ | Φ | Φ | | Φ | Φ | Φ | Φ | F,G, BP-I-A/B |
| Dasatinib-Abl | 2gqg | | | Φ | | Φ | Φ, A | Φ | | Φ | Φ | Φ | Φ | F, G, B, BP-I-A/B |
| Erlotinib-EGFR | 1m17 | | | | | | Φ | Φ | | Φ | Φ | Φ | Φ | F, G, B, BP-I-A/B |
| Gefitinib-EGFR | 2ity | | | Φ | | | Φ | Φ | | Φ | Φ | Φ | Φ | F,G, BP-I-A/B |
| Palbociclib-CDK6 | 2euf | | | | | Φ | Φ | | | Φ | Φ | Φ | Φ | F |
| Pralsetinib-RET | 7ju5 | | | | | | Φ | | | Φ | Φ | Φ | Φ | F, FP-II |
| R406 (fostamatinib) | 3fqs | | | | | Φ | Φ | | | Φ | Φ | Φ | Φ | F |
| Selpercatinib-RET | 7ju6 | | | | | | Φ | | | Φ | Φ | Φ | Φ | F, FP-II |
| Vandetanib-RET | 2ivu | | | | Φ | Φ | Φ | Φ | | Φ | Φ | Φ | Φ | F,G, BP-I-A/B |
| *Type I½A inhibitors* | | | | | | | | | | | | | | |
| Dabrafenib–B-Raf | 5csw | | Φ, D | Φ | Φ | Φ | Φ | Φ | | Φ | Φ | Φ | Φ | F, G, B, FP-II, BP-I-A/B, BP-II-in, BP-II-A-in |
| Erdafitinib-FGFR1 | 5ew8 | | Φ | Φ | | Φ | Φ | Φ | | Φ | Φ | Φ | Φ | F, G, B, FP-I, BP-I-A/B |
| **Infigratinib**-FGFR1 | 3tt0 | | | Φ | | Φ | Φ | Φ | | Φ | Φ | Φ | Φ | F, G, B, BP-I-A/B |
| Lapatinib-EGFR | 1xkk | | Φ | Φ | Φ | Φ | Φ | Φ | | Φ | Φ | Φ | Φ | F, G, B, BP-I-A/B, BP-II-in, BP-II-A-in |
| Lenvatinib-VEGFR | 3wzd | | Φ | Φ | | Φ | Φ | | | Φ | Φ | Φ | Φ | F, G, B, BP-I-B, BP-II-in |
| Vemurafenib-B-Raf | 3og7 | | Φ | Φ | Φ | Φ | Φ | Φ | | Φ | Φ | Φ | Φ | F, G, B, FP-I, BP-I-A/B, BP-II-in, BP-II-A-in |
| *Type I½B inhibitors* | | | | | | | | | | | | | | |
| Abemeciclib-CDK6 | 5l2s | | | | | Φ | Φ | | | Φ | Φ | Φ | Φ | F, FP-II |
| Alectinib-ALK | 3aox | | | | | Φ | Φ | | | Φ | Φ | Φ | Φ | F, BP-I-B |
| Brigatinib-ALK | 6mx8 | | | | | | Φ | | | Φ | Φ | Φ | Φ | F, FP-I |
| Ceritinib-ALK | 4mkc | | | | | | | | | Φ | Φ | Φ | Φ | F, FP-I |
| Crizotinib-ALK | 2xp2 | | | | | | Φ | | | Φ | Φ | Φ | Φ | F, FP-I |
| Crizotinib-MET | 2wgj | | | | | Φ | Φ | | | Φ | Φ | Φ | Φ | F, FP-I |
| Crizotinib-ROS1 | 3zbf | | | | | Φ | Φ | | | Φ | Φ | Φ | Φ | F, FP-I |
| Entrectinib-TRKA | 5kvt | | | | | Φ | Φ | | Φ | Φ | Φ | Φ | Φ | F, FP-I |
| Erlotinib-EGFR | 4hjo | | | Φ | | Φ | Φ | | | Φ | Φ | Φ | Φ | F, G, BP-I-A/B |
| Lorlatinib-ALK | 4cli | | | | | | | | | Φ | Φ | Φ | Φ | F, FP-I |
| Palbociclib-CDK6 | 2l2i | | | | | Φ | Φ | | | Φ | Φ | Φ | Φ | F |
| Ribociclib-CDK6 | 5l2t | | | | | Φ | Φ | | | Φ | Φ | Φ | Φ | F, G, FP-I |
| **Tepotinib**-MET | 4r1v | | | | | Φ | Φ | | | Φ | Φ | Φ | Φ | F, FP-I |
| Tofacitinib-JAK1 | 3eyg | | | | | Φ | Φ | | | Φ | Φ | Φ | Φ | F, FP-I/II |
| Tofacitinib-JAK3 | 3lxk | | | | | Φ | Φ | | Φ | Φ | Φ | Φ | Φ | F, FP-I/II |
| *Type IIA inhibitors* | | | | | | | | | | | | | | |
| Axitinib-VEGFR | 4ag8 | | Φ | Φ | | Φ | Φ | Φ | | Φ | Φ | Φ | Φ | F, G, B, BP-I-B, BP-II-out |
| Imatinib-Abl[f] | 1iep | Φ, A | Φ | Φ | | Φ | Φ, A | Φ | | Φ | Φ | Φ | Φ | F, G, B, BP-I-A/B, BP-II-out, BP-IV |
| Imatinib-Kit | 1t46 | Φ | Φ | Φ | | Φ | Φ, A | Φ | | Φ | Φ | Φ | Φ | F, G, B, BP-I-A/B, BP-II-out, BP-IV |
| Nilotinib-Abl | 3cs9 | Φ | Φ | Φ | | Φ | Φ, A | Φ | | Φ | Φ | Φ | Φ | F, G, B, BP-I-A/B, BP-II-out, BP-III, BP-V |
| Pexidartinib-CSF1R | 4r7h | | Φ | Φ | | Φ | Φ | | | Φ | Φ | Φ | Φ | F, G, B, BP-I-B, BP-II-out, BP-V |
| Ponatinib-Abl[f] | 3oxz | Φ, A | Φ | Φ | | Φ | Φ | Φ | | Φ | Φ | Φ | Φ | F, G, B, BP-I-A/B, BP-II-out, BP-III, BP-IV |
| Ponatinib-Kit | 4u0i | Φ, A | Φ | Φ | | Φ | Φ | Φ | | Φ | Φ | Φ | Φ | F, G, B, BP-II-A/B, BP-II-out, BP-III, BP-IV |
| Ripretinib-Kit | 6mob | Φ | Φ | Φ | | Φ | Φ | Φ | | Φ | Φ | Φ | Φ | F, G, B, BP-I-A/B, BP-II-out, BP-III |
| Sorafenib-CDK8 | 3rgf | Φ | Φ | Φ | | Φ | Φ | | | Φ | Φ | Φ | Φ | F, G, B, BP-I-B, BP-II-out, BP-III |
| Sorafenib-VEGFR | 4asd | Φ | Φ | Φ | | Φ | Φ | | | Φ | Φ | Φ | Φ | F, G, B, BP-I-B, BP-II-out, BP-III |
| **Tivozanib**-VEGFR2 | 4ase | | Φ | Φ | | Φ | Φ | Φ | | Φ | Φ | Φ | Φ | F, G, B, BP-I-B, BP-II-out |
| *Type IIB inhibitors* | | | | | | | | | | | | | | |
| Bosutinib-Abl | 3ue4 | | Φ | Φ | | Φ | Φ | Φ | | Φ | Φ | Φ | Φ | F, G, BP-II-A/B |
| Gilteritinib-FLT3 | 6jqr | | Φ | | | | | | | Φ | Φ | Φ | Φ | F |
| Nintedanib-VEGFR2 | 3c7q | | | Φ | | Φ | Φ | | | Φ | Φ | Φ | Φ | F, G, BP-I-B |
| Sunitinib-Kit | 3g0e | | Φ | | | Φ | | | | Φ | Φ | Φ | Φ | F |
| Sunitinib-VEGFR | 4agd | | Φ | | | Φ | Φ | | | Φ | Φ | Φ | Φ | F, BP-I-B |
| *Type III inhibitors* | | | | | | | | | | | | | | |
| Cobimetinib-MEK1 | 4an2 | | Φ | | | Φ | Φ | Φ | | | | | | G, B, BP-II-in |
| Selumetinib-MEK1 | 4u7z | | Φ | | | Φ | Φ | Φ | | | | | | G, B, BP-II-in |
| *Type VI inhibitors* | | | | | | | | | | | | | | |
| Afatinib-EGFR | 4g5j | | | Φ | | | Φ | Φ | | Φ | Φ | Φ | Φ | F, G, BP-I-A/B |
| Dacomitinib-EGFR | 4i24 | | | | | | Φ | Φ | | Φ | Φ | Φ | Φ | F, G, BP-I-B |
| Ibrutinib-BTK | 5p9j | | Φ | Φ | | Φ | Φ | Φ | | Φ | Φ | Φ | Φ | F, G, B, BP-I-B |
| Neratinib-EGFR | 2jiv | | Φ | Φ | Φ | Φ | Φ | Φ | | Φ | Φ | Φ | Φ | F, G, B, BP-I-A/B |
| Osimertinib-EGFR | 6jxt | | | | | | | | | Φ | Φ | Φ | Φ | F |
| Zanubrutinib-BTK | 6j6m | | Φ | Φ | | Φ | Φ | Φ | | Φ | Φ | Φ | Φ | F, G, B, BP-I-B |

[a] klifs.net.
[b] Human enzyme unless otherwise noted.
[c] Drugs not previously reviewed (Refs [10–12]) are indicated in **bold** print.
[d] KLIFS-3, kinase-ligand interaction fingerprint and structure residue-3.
[e] A, hydrogen-bond acceptor; D, hydrogen-bond donor.
[f] Mouse enzyme

Unfortunately, up to 70% of patients require additional lines of therapy. The Bruton tyrosine kinase inhibitor ibrutinib was also FDA-approved in 2017 for the treatment of graft vs. host disease and the addition of belumosudil provides an additional option.

Mobocertinib is an indole-pyrimidine derivative (Fig. 4E) that is FDA-approved for the treatment of NSCLC that contains EGFR exon 20 insertions [80,81]. Afatinib, dacomitinib, erlotinib, gefitinib, and osimertinib, which are FDA-approved EGFR/ErbB1 inhibitors used for the treatment of NSCLC, are not effective in the treatment of lung cancers bearing these mutations. Exon 20 insertions represent about 4–12% of *EGFR* mutations that occur in NSCLC and mobocertinib is the only approved medicinal that specifically targets these mutants. These insertions occur between amino acid 767 and 774 near the C-terminus of the αC-helix. This antagonist was designed to inhibit oncogenic variants containing mutations in exon 20 with selectivity over the wildtype enzyme. The mobocertinib isopropyl ester was designed to interact specifically with the gatekeeper residue (T790) of these mutants. The $IC_{50}$ in cells with wildtype EGFR was about 35 nM and the average for cells bearing various exon 20 insertions was about 10 nM [80]. Mobocertinib was designed to form a covalent bond with C797 of EGFR. Studies of cells bearing EGFR lacking this residue were resistant to the action of this drug providing confirmatory data on the proposed mechanism of action of this compound. See Refs. [80,81] for a summary of the clinical trials that led to the approval of this type VI [31] irreversible inhibitor.

Trilaciclib is a tetraza-aminopyridine derivative (Fig. 4F) that inhibits CDK4/6 that is used to decrease the incidence of chemotherapy-induced myelosuppression in adults when administered prior to a platinum/etoposide-containing regimen or a topotecan-containing regimen for extensive-stage small cell lung cancer [82,83]. Cyclins and cyclin-dependent protein kinases (CDKs) are important proteins that are required for the regulation and expression of the large number of components necessary for the passage through the cell cycle. The concentrations of the CDKs are generally constant, but their activities are controlled by the oscillation of the cyclin levels during each cell cycle. In response to mitogenic stimuli, cells in the G1-phase of the cell cycle produce D type cyclins that activate CDK4/6. These activated enzymes catalyze the monophosphorylation of the retinoblastoma protein. This cancer is rapidly growing with an 8-to-13-month median survival. CDK4/6 inhibitors may shield both hematopoietic stem cells and cancer cells from the toxicity of chemotherapy. This problem is avoided in small cell lung cancers because of the chemosensitivity of these malignancies and the absence of the retinoblastoma (RB) tumor suppressor protein in most of these neoplasms. Chemotherapy-induced damage of hematopoietic stem and progenitor cells causes generalized myelosuppression.

Trilaciclib treatment is hypothesized to preserve hematopoietic stem and progenitor cells and immune system function during chemotherapy (myelopreservation). Intravenous trilaciclib transiently maintains these stem and progenitor cells in G1 arrest and protects them from cytotoxic damage, leading to more rapid cellular recovery and enhanced antitumor immunity. Weiss et al. reported that trilaciclib reduced both the occurrence and duration of severe neutropenia. Improvement in neutrophil and erythrocyte endpoints were also observed with a delayed hemoglobin decline and a faster recovery of lymphocytes. Moreover, there was a reduction in the number of therapeutic blood transfusions. These investigators reported that the CDK4/6 inhibitor did not lower the efficacy of chemotherapy. Powell and Prasad wrote that additional evidence from larger Phase III trials should be performed to confirm the efficacy of trilaciclib in the treatment of this disorder [83].

## 6. Physicochemical properties of orally effective drugs

### 6.1. Lipinski's rule of five (Ro5)

Pharmacologists and medicinal chemists have sought the physicochemical properties that result in drugs that are orally bioavailable. Lipinski's rule of five (Ro5) is a computational and experimental methodology that is used to characterize membrane permeability, solubility, and efficacy in the drug-development setting [84]. It is a rule of thumb that evaluates drug-likeness and establishes whether an agent with specific pharmacological activities has properties suggesting that it would be orally effective. The Lipinski criteria were grounded on data demonstrating that most orally effective medicines are comparatively small and moderately lipophilic molecules. The Ro5 criteria are used during drug development as biologically active lead compounds are serially optimized to increase their activity while maintaining selectivity and drug-like properties.

The Ro5 implies that less than ideal oral bioavailability is more likely to occur when (i) the atom-based calculated Log P (ALogP) is greater than 5, when (ii) there are more than 5 hydrogen-bond donors, when (iii) there are more than $5 \times 2$ or 10 hydrogen-bond acceptors, and when (iv) the molecular weight is more than $5 \times 100$ or 500 [84]. The partition coefficient (P) is the ratio of the solubility of the un-ionized drug in the organic phase of water-saturated *n*-octanol divided by its solubility in the aqueous phase. The P value reflects the hydrophobicity of a drug; the larger the P value, the greater the hydrophobicity. The number of hydrogen-bond donors is easy to calculate and is the sum of NH and OH groups. The number of hydrogen-bond acceptors is more difficult to assess as it consists of any neutral heteroatom with the exception of pyrrole nitrogen atoms, halogen atoms, heteroaromatic oxygen and sulfur atoms, and higher oxidation states of nitrogen, phosphorus, and sulfur, but it includes the oxygen atoms bonded to them. The Ro5 is based on the physicochemical properties of more than two thousand reference drugs [84].

Excluding the macrolides (everolimus, sirolimus, and temsirolimus), the average molecular weight (MW) of the orally effective FDA-approved protein kinase inhibitors is 482 ranging from 306 (ruxolitinib) to 615 (trametinib) (Table 8). The compounds with a molecular weight greater than 500 include the three macrolides, the newly approved infigratinib and mobocertinib, and 22 other drugs. Although this data indicates that there is a propensity for orally bioavailable small molecule protein kinase antagonists to exceed the 500 Da molecular-weight criterion, the masses of the larger compounds are still near 500 Da. Moreover, 23 of the 68 approved drugs have an ALogP of greater than five including the newly approved mobocertinib, infigratinib, and tivozanib. In addition, gefitinib and belumosudil have more than five hydrogen bond donors and mobocertinib, infigratinib, fedratinib, baricitinib, and palbociclib have more than ten hydrogen bond acceptors. Overall, a total of 28 of the 68 FDA-approved small molecule protein kinase inhibitors fail to conform to Lipinski's Ro5. Of these 28, only the orally bioavailable and newly approved mobocertinib and infigratinib have two Ro5 deficiencies with a molecular weight greater than 500 and a partition coefficient greater than 5. These are FDA-approved drugs, but finding drug candidates during development with two Ro5 criteria exceptions is usually an undesirable result.

### 6.2. The importance of lipophilicity and ligand efficiency

#### 6.2.1. Lipophilic efficiency, LipE

After the emergence of Lipinski's Ro5 in 2001 [84], subsequent work on the physical and chemical properties of orally bioavailable medicines has led to various refinements [85–92]. For example, lipophilic efficiency, or LipE, is a property that is used in drug discovery and development that combines potency and lipophilic-driven binding as a strategy to increase binding efficacy. The following formulas are used to compute lipophilic efficiency:

$$\text{LipE} = \text{p}IC_{50} - \text{ALogP};\ \text{LipE} = \text{p}K_i - \text{ALogP}$$

Like its usage to express the molar hydrogen ion concentration as pH, the operator p denotes the negative of the $\text{Log}_{10}$ of the $IC_{50}$ or $K_i$. Furthermore, ALogP is an atom-based computed $\text{Log}_{10}$ of the partition

**Table 8**
Properties of FDA-approved small molecule inhibitors [a].

| Drug | Pubchem CID | Formula | MW (Da) | HD[b] | HA[c] | ALogP[a,d] | Rotatable bonds | PSA[e] (Å$^2$) | Ring Count[f] | Complexity[g] |
|---|---|---|---|---|---|---|---|---|---|---|
| Abemaciclib | 46220502 | $C_{27}H_{32}F_2N_8$ | 507 | 1 | 9 | 4.94 | 7 | 75 | 5 | 723 |
| Acalabrutinib | 71226662 | $C_{26}H_{23}N_7O_2$ | 466 | 2 | 6 | 3.31 | 4 | 119 | 5 | 845 |
| Afatinib | 10184653 | $C_{24}H_{25}ClFN_5O_3$ | 486 | 2 | 8 | 4.39 | 8 | 88.6 | 4 | 702 |
| Alectinib | 49806720 | $C_{30}H_{34}N_4O_2$ | 483 | 1 | 5 | 4.77 | 3 | 72.4 | 6 | 867 |
| Avapritinib | 118023034 | $C_{26}H_{27}FN_{10}$ | 499 | 1 | 9 | 2.61 | 5 | 106 | 6 | 752 |
| Axitinib | 6450551 | $C_{22}H_{18}N_4OS$ | 386 | 2 | 4 | 4.64 | 5 | 96 | 4 | 557 |
| Baricitinib | 44205240 | $C_{16}H_{17}N_7O_2S$ | 371 | 1 | 7 | 1.10 | 5 | 129 | 4 | 678 |
| **Belumosudil** | 11950170 | $C_{26}H_{24}N_6O_2$ | 452 | 3 | 6 | 4.82 | 7 | 105 | 5 | 678 |
| Binimetinib | 10288191 | $C_{17}H_{15}BrF_2N_4O_3$ | 441 | 3 | 7 | 3.01 | 6 | 88.4 | 3 | 521 |
| Bosutinib | 5328940 | $C_{26}H_{29}Cl_2N_5O_3$ | 530 | 1 | 8 | 5.19 | 9 | 82.9 | 4 | 734 |
| Brigatinib | 68165256 | $C_{29}H_{39}ClN_7O_2P$ | 584 | 2 | 9 | 5.09 | 8 | 85.9 | 5 | 835 |
| Cabozantinib | 25102847 | $C_{28}H_{24}FN_3O_5$ | 501 | 2 | 7 | 5.54 | 8 | 98.8 | 4 | 795 |
| Capmatinib | 25145656 | $C_{23}H_{17}FN_6O$ | 412 | 1 | 6 | 3.43 | 5 | 81.5 | 5 | 637 |
| Ceritinib | 57379345 | $C_{28}H_{36}ClN_5O_3S$ | 558 | 3 | 8 | 6.36 | 9 | 114 | 4 | 835 |
| Cobimetinib | 16222096 | $C_{21}H_{21}F_3IN_3O_2$ | 531 | 3 | 7 | 3.78 | 4 | 64.6 | 4 | 624 |
| Crizotinib | 11626560 | $C_{21}H_{22}Cl_2FN_5O$ | 450 | 2 | 6 | 5.04 | 5 | 78 | 4 | 558 |
| Dabrafenib | 44462760 | $C_{23}H_{20}F_3N_5O_2S_2$ | 520 | 2 | 11 | 5.36 | 6 | 148 | 4 | 817 |
| Dacomitinib | 11511120 | $C_{24}H_{25}ClFN_5O_2$ | 470 | 2 | 7 | 5.16 | 7 | 79.4 | 4 | 665 |
| Dasatinib | 3062316 | $C_{22}H_{26}ClN_7O_2S$ | 488 | 3 | 9 | 3.31 | 7 | 135 | 4 | 642 |
| Encorafenib | 50922675 | $C_{22}H_{27}ClFN_7O_4S$ | 540 | 3 | 10 | 3.91 | 10 | 149 | 3 | 836 |
| Entrectinib | 25141092 | $C_{31}H_{34}F_2N_6O_2$ | 561 | 3 | 8 | 5.03 | 7 | 85.5 | 6 | 847 |
| Erdafitinib | 67462786 | $C_{25}H_{30}N_6O_2$ | 446 | 1 | 7 | 4.18 | 9 | 77.3 | 4 | 583 |
| Erlotinib | 176870 | $C_{22}H_{23}N_3O_4$ | 393 | 1 | 7 | 3.41 | 11 | 74.7 | 3 | 525 |
| Everolimus | 6442177 | $C_{53}H_{83}NO_{14}$ | 958 | 3 | 14 | 6.20 | 9 | 205 | 3 | 1810 |
| Fedratinib | 16722836 | $C_{27}H_{36}N_6O_3S$ | 525 | 3 | 9 | 4.82 | 11 | 117 | 4 | 787 |
| Fostamatinib | 11671467 | $C_{23}H_{26}FN_6O_9P$ | 580 | 4 | 15 | 3.09 | 10 | 187 | 4 | 904 |
| Gefitinib | 123631 | $C_{22}H_{24}ClFN_4O_3$ | 447 | 1 | 8 | 4.28 | 8 | 68.7 | 4 | 545 |
| Gilteritinib | 49803313 | $C_{29}H_{44}N_8O_3$ | 552 | 3 | 10 | 2.70 | 9 | 121 | 5 | 785 |
| Ibrutinib | 24821094 | $C_{25}H_{24}N_6O_2$ | 441 | 1 | 6 | 4.22 | 5 | 99.2 | 5 | 678 |
| Imatinib | 5291 | $C_{29}H_{31}N_7O$ | 494 | 2 | 7 | 4.59 | 7 | 86.3 | 5 | 706 |
| **Infigratinib** | 53235510 | $C_{26}H_{31}Cl_2N_7O_3$ | 560 | 2 | 8 | 5.35 | 8 | 95.1 | 4 | 724 |
| Lapatinib | 208908 | $C_{29}H_{26}ClN_4O_4S$ | 580 | 2 | 9 | 6.14 | 11 | 115 | 5 | 898 |
| Larotrectinib | 46188928 | $C_{21}H_{22}F_2N_6O_2$ | 428 | 2 | 7 | 2.95 | 3 | 86 | 5 | 659 |
| Lenvatinib | 9823820 | $C_{21}H_{19}ClN_4O_4$ | 427 | 3 | 5 | 4.07 | 6 | 116 | 4 | 634 |
| Lorlatinib | 71731823 | $C_{21}H_{19}FN_6O_2$ | 406 | 1 | 7 | 2.80 | 0 | 110 | 3 | 700 |
| Midostaurin | 9829523 | $C_{35}H_{30}N_4O_7$ | 571 | 1 | 4 | 5.91 | 3 | 77.7 | 5 | 1140 |
| **Mobocertinib** | 118607832 | $C_{32}H_{39}N_7O_4$ | 586 | 2 | 9 | 5.08 | 13 | 114 | 4 | 881 |
| Neratinib | 9915743 | $C_{30}H_{29}ClN_6O_3$ | 557 | 2 | 8 | 5.93 | 11 | 112 | 4 | 881 |
| Netarsudil | 66599893 | $C_{28}H_{27}N_3O_3$ | 454 | 2 | 5 | 4.89 | 8 | 94.3 | 4 | 678 |
| Nilotinib | 644241 | $C_{28}H_{22}F_3N_7O$ | 530 | 2 | 9 | 6.36 | 6 | 97.6 | 5 | 817 |
| Nintedanib | 135423438 | $C_{31}H_{33}N_5O_4$ | 540 | 2 | 7 | 3.62 | 8 | 102 | 5 | 947 |
| Osimertinib | 71496458 | $C_{28}H_{33}N_7O_2$ | 500 | 2 | 7 | 4.51 | 10 | 87.6 | 4 | 752 |
| Palbociclib | 5330286 | $C_{24}H_{29}N_7O_2$ | 448 | 2 | 8 | 2.97 | 5 | 103 | 5 | 775 |
| Pazopanib | 10113978 | $C_{21}H_{23}N_7O_2S$ | 438 | 2 | 8 | 3.14 | 5 | 127 | 4 | 717 |
| Pemigatinib | 86705659 | $C_{24}H_{27}F_2N_5O_4$ | 487 | 2 | 7 | 3.66 | 6 | 88.4 | 5 | 731 |
| Pexidartinib | 25151352 | $C_{20}H_{15}ClF_3N_5$ | 417 | 2 | 7 | 5.23 | 5 | 66.5 | 4 | 537 |
| Ponatinib | 24826799 | $C_{29}H_{27}F_3N_6O$ | 533 | 1 | 8 | 4.46 | 6 | 65.8 | 5 | 910 |
| Pralsetinib | 129073603 | $C_{27}H_{32}FN_9O_2$ | 534 | 3 | 9 | 4.20 | 8 | 136 | 5 | 816 |
| Regorafenib | 11167602 | $C_{21}H_{15}ClF_4N_4O_3$ | 483 | 3 | 8 | 5.69 | 5 | 92.4 | 3 | 686 |
| Ribociclib | 44631912 | $C_{23}H_{30}N_8O$ | 435 | 2 | 7 | 2.80 | 5 | 91.2 | 5 | 636 |
| Ripretinib | 71584930 | $C_{24}H_{21}BrFN_5O_2$ | 510 | 3 | 5 | 5.67 | 5 | 86.4 | 4 | 746 |
| Ruxolitinib | 25126798 | $C_{17}N_{18}N_6$ | 306 | 1 | 4 | 3.47 | 4 | 83.2 | 4 | 453 |
| Selpercatinib | 134436906 | $C_{29}H_{31}N_7O_3$ | 526 | 1 | 9 | 3.28 | 8 | 112 | 6 | 637 |
| Selumetinib | 10127622 | $C_{17}H_{15}BrClF_4O_3$ | 458 | 3 | 6 | 3.53 | 6 | 88.4 | 3 | 523 |
| Sirolimus | 5284616 | $C_{51}H_{79}NO_{13}$ | 914 | 3 | 13 | 6.18 | 6 | 195 | 3 | 1760 |
| Sorafenib | 216239 | $C_{21}H_{16}ClF_3N_4O_3$ | 465 | 3 | 7 | 5.55 | 5 | 92.4 | 3 | 646 |
| Sunitinib | 5329102 | $C_{22}H_{27}FN_4O_2$ | 398 | 3 | 4 | 3.33 | 7 | 77.2 | 3 | 636 |
| Temsirolimus | 6918289 | $C_{56}H_{87}NO_{16}$ | 1029 | 4 | 16 | 4.39 | 11 | 242 | 3 | 2010 |
| **Tepotinib** | 25171648 | $C_{29}H_{28}N_6O_2$ | 493 | 7 | 7 | 4.01 | 7 | 94.7 | 5 | 880 |
| **Tivozanib** | 9911830 | $C_{22}H_{19}CLIN_4O_5$ | 455 | 2 | 6 | 5.64 | 6 | 108 | 4 | 631 |
| Tofacitinib | 9926791 | $C_{16}H_{20}N_6O$ | 312 | 1 | 5 | 1.54 | 3 | 88.9 | 3 | 488 |
| Trametinib | 11707110 | $C_{26}H_{23}FIN_5O_4$ | 615 | 2 | 6 | 3.94 | 5 | 102 | 4 | 1090 |
| **Trilaciclib** | 68029832 | $C_{24}H_{30}N_8O$ | 447 | 2 | 7 | 2.72 | 3 | 91.2 | 6 | 707 |
| Tucatinib | 51039094 | $C_{26}H_{24}N_8O_2$ | 481 | 2 | 8 | 5.09 | 6 | 111 | 6 | 796 |
| Upadacitinib | 58557659 | $C_{17}H_{19}F_3N_6O$ | 380 | 2 | 6 | 2.91 | 3 | 78.3 | 4 | 561 |
| Vandetanib | 3081361 | $C_{22}H_{24}BrFN_4O_2$ | 475 | 1 | 7 | 5.00 | 6 | 59.5 | 4 | 539 |
| Vemurafenib | 42611257 | $C_{23}H_{18}ClF_2N_3O_3S$ | 490 | 2 | 7 | 5.54 | 7 | 100 | 4 | 790 |
| Zanubrutinib | 135565884 | $C_{27}H_{27}N_5O_3$ | 472 | 2 | 5 | 4.22 | 6 | 103 | 5 | 756 |

[a] Drugs previously not reviewed (Refs. [10–12]) are given in **bold** type.
[b] No. of hydrogen bond donors.
[c] No. of hydrogen bond acceptors.
[d] Values for atom-based log of the partition coefficient (ALogP) from https://www.ebi.ac.uk/chembl/.
[e] PSA, polar surface area.

[f] Includes aromatic and nonaromatic rings.
[g] Values obtained from https://pubchem.ncbi.nlm.nih.gov/.

coefficient; this parameter denotes the ratio of the drug solubility in the organic phase divided by its solubility in the aqueous phase of immiscible *n*-octanol/water.

The second term of the equation (– ALogP or minus ALogP) reflects the lipophilicity of a medicinal and the value is computed using an algorithm based upon the properties of thousands of reference organic compounds. The greater the solubility of a compound in the organic phase of the two phase *n*-octanol/water mixture, the greater is its lipophilicity. Leeson and Springthorpe hypothesized that drug lipophilicity, as assessed by its – ALogP value, is one of the more important properties that should be checked during drug development [86]. Their use of – ALogP was based upon studies conducted before the use of the distribution coefficient (D) became more common. The distribution coefficient ($LogD_{7.4}$) is the ratio of the solubility of the ionized and un-ionized drug in the organic phase and the aqueous phase of immiscible *n*-octanol/water at a specified pH of the aqueous phase, which is usually 7.4. For practical purposes, either ALogP or LogD can be used to compare a series of several compounds in the same study. Note that an agent with a large lipophilicity and a large negative (– ALogP) value decreases the lipophilic efficiency.

A high lipophilicity may facilitate the binding of a drug to adventitious targets that may augment toxicity and adverse events. One objective for developing advantageous properties during drug discovery is to increase potency without simultaneously increasing lipophilicity. Lipophilic efficiency helps in the optimization of lead compounds by allowing a direct comparison of a series of drug congeners; moreover, the same assay should be used to ensure that such comparisons are valid [88,89]. To cite one successful example, progress in the optimization of lead compounds during the development of crizotinib as described by Cui et al. was monitored by using lipophilic efficiency as an index of binding effectiveness [93]; crizotinib is FDA-approved for the treatment of ALK-positive and ROS1-positive NSCLC.

ALogP of related compounds can be computed in a matter of minutes. Because experimental determinations of LogP are labor intensive, such measurements are performed in only select cases. Hopkins et al. suggested that acceptable values of lipophilic efficiency are greater than ~ 5 and those for LogP are less than ~ 3 [88]. Decreasing the lipophilicity and increasing potency during drug development generally produces medicines with better pharmacological properties. The average value of lipophilic efficiency (LipE) for 65 FDA-approved small molecule protein kinase inhibitors (omitting the macrolides) is 4.29 with a range from 1.3 (neratinib) to 7.56 (tofacitinib) and a standard deviation of 1.44 (Table 9). The average value for ALogP for the 65 FDA-approved drugs was 4.32 with a standard deviation of 1.18.

### 6.2.2. Ligand efficiency, LE

The ligand efficiency (LE) relates binding affinity, or potency, to the number of heavy (nonhydrogen) atoms of a medicine. The following formula is used to calculate this property:

$$LE = \Delta G^{\circ\prime}/N = -RT \ln K_{eq}/N = -2{\cdot}303RT \text{ Log } K_{eq}/N$$

$\Delta G^{\circ\prime}$ is the standard free energy change of a ligand binding to its target enzyme at neutral pH, R represents the energy-temperature coefficient or universal gas constant, ($1.98 \times 10^{-3}$ kcal/degree-mol), T signifies the absolute temperature in degrees Kelvin, $K_{eq}$ is the value of the equilibrium constant, and N represents the number of heavy (nonhydrogen) atoms in the ligand. Hopkins et al. reported that optimal values of ligand efficiency exceed 0.3 kcal/mol [85,88]. The $K_{i \text{ or }} IC_{50}$ values are proxies for the equilibrium constant. At a physiological temperature of 37 °C (310 K), this equation becomes – ($2.303 \times (1.98 \times 10^{-3}$/K) × 310 K Log $K_{eq}$)/N or – 1.41 Log $K_{eq}$/N. Other authors use a temperature of 300 K and the multiplication factor is – 1.37 [88,92]. Ligand efficiency is a procedure for comparing ligand affinities based upon the average binding energy per atom. Moreover, ligand efficiency is especially useful in fragment-based drug discovery protocols and, like lipophilic efficiency, it helps in the selection of derivatives of lead compounds for further development [89].

Ligand efficiency corresponds to the binding affinity per heavy atom of the drug or ligand of interest. The value of N is a proxy for the molecular weight. The equation that describes ligand efficiency reveals that the value is directly proportional to – Log $K_{eq}$ (a positive number), or the binding affinity, and is inversely proportional to the number of heavy atoms. Hopkins et al. suggested that optimal values for ligand efficiency (LE) should be greater than 0.3 kcal per mol per heavy atom [88]. The values of ligand efficiency for the FDA-approved small molecule protein kinase inhibitors based upon representative $K_i$ or $IC_{50}$ values are provided in Table 9. The average value for ligand efficiency for 65 of the FDA-approved protein kinase inhibitors (excluding the three macrolides) was 0.360 and a standard deviation of 0.06. Six drugs had values of less than 0.3 including fostamatinib, nilotinib, nintedanib, neratinib, midostaurin, and mobocertinib with the lowest value of 0.237. The values for lipophilic efficiency (LipE) and ligand efficiency (LE) listed in Table 9 are based on data acquired under different experimental conditions. Accordingly, these values cannot be used to make a direct comparison of the medicinals owing to the different assay conditions that were used to obtain the data. These results were obtained from different drug discovery projects and are meant to provide representative values. The main protein kinase families that are targeted by the FDA-approved drugs are also listed in Table 9.

### 6.2.3. Additional chemical descriptors of orally effective drugs

To improve drug properties related to oral bioavailability, not-unexpectedly, the Ro5 has generated many additions and corollaries. For example, Veber et al. reported that the number of rotatable bonds and the polar surface area (PSA) differentiates between orally active and inactive agents for a large series of substances in rats [90]. They reported that the optimal number of rotatable bonds should be 10 or less. This property is believed to control passive membrane permeation and reflects molecular flexibility (degrees of freedom). Furthermore, the number of degrees of freedom correlates with the entropy change that accompanies ligand binding and determines in part the extent of drug binding to its targets. With the exceptions of four drugs with 11 rotatable bonds (neratinib, erlotinib, lapatinib and temsirolimus) and the newly approved mobocertinib with 13 rotatable bonds, the remaining 63 drugs have 10 or fewer of these bonds. The average value is 6.6 and the number of rotatable bonds ranges from 0 (lorlatinib) to 13 (mobocertinib). Moreover, these authors stated that medicines with polar surface area values less than or equal to 140 $Å^2$ are orally bioavailable. This parameter represents the sum of the surface over all polar atoms, primarily nitrogen and oxygen, but it also includes any linked hydrogen atoms. With the exceptions of seven drugs (dabrafenib, encorafenib, fostamatinib, the three macrolides, and the newly approved mobocertinib), the other 61 medicines have a polar surface area less than 140 $Å^2$; the average value is 103 with a range from 59.5 (vandetanib) to 242 (temsirolimus) (Table 8). Moreover, Oprea found that the number of rings (both aromatic and nonaromatic) in most orally approved drugs is three or greater [91]. All of the approved small molecule protein kinase inhibitors have three or more rings with an average value of 4.26 and a range from three to six. All of the FDA-approved drugs listed are orally effective with the exceptions of temsirolimus and trilaciclib (which are given intravenously) and netarsudil (an eye drop). Furthermore, ruxolitinib is effective orally and topically.

The molecular complexity of a compound is based upon the elements it contains, its structural features, and any symmetry elements. The complexity is computed using the Bertz/Hendrickson/Ihlenfelt

**Table 9**
Properties of FDA-approved small molecule inhibitors [a].

| Drug | Target, kinase family[b] | $K_i$ nM[c] | p$K_i$ | ALogP[d] | LipE[e] | N[f] | LE[g] | Dosage, mg/day[h] | Solubility[i], μg/ml | Log $D_{7.4}$[c] | nRb[j] | nAr[k] | Benzenes | QED[l] |
|---|---|---|---|---|---|---|---|---|---|---|---|---|---|---|
| Abemaciclib | CDK4, S/T | 0.6 | 9.22 | 4.94 | 4.28 | 37 | 0.351 | 400 * | 15.9 | 3.76 | 7 | 4 | 0 | 0.38 |
| Acalbrutinib | BTK, NRY | 3.1 | 8.51 | 3.31 | 5.20 | 35 | 0.343 | 200 * | 10.9 | 2.56 | 4 | 4 | 1 | 0.45 |
| Afatinib | EGFR, RY | 0.5 | 9.33 | 4.39 | 4.94 | 34 | 0.387 | 40 | 12.8 | 2.34 | 8 | 3 | 1 | 0.46 |
| Alectinib | ALK, RY | 1.9 | 8.72 | 4.77 | 3.95 | 36 | 0.342 | 1200 * | 10.5 | 4.75 | 3 | 3 | 0 | 0.58 |
| Avapritinib | PDGFRα, RY | 0.18 | 9.7 | 2.61 | 7.09 | 37 | 0.370 | 300 | 30.1 | 2.12 | 5 | 5 | 1 | 0.39 |
| Axitinib | VEGFR2, RY | 0.25 | 9.6 | 4.64 | 4.96 | 28 | 0.483 | 300 | 0.55 | 4.15 | 5 | 4 | 1 | 0.52 |
| Baricitinib | JAK2, NRY | 7 | 8.15 | 1.1 | 7.05 | 26 | 0.442 | 2 | 357 | -0.19 | 5 | 3 | 0 | 0.72 |
| **Belumosudil** | ROCK2, S/T | 53.9 | 7.3 | 4.82 | 2.48 | 34 | 0.303 | 200 | 2.89 | 4.02 | 7 | 5 | 1 | 0.33 |
| Binimetinib | MEK1, DS | 12 | 7.92 | 3.01 | 4.91 | 27 | 0.414 | 90 * | 49.9 | 3.81 | 6 | 3 | 1 | 0.40 |
| Bosutinib | BCR-Abl, NRY | 20 | 7.7 | 5.19 | 2.51 | 36 | 0.302 | 500 | 9.5 | 3.37 | 9 | 3 | 1 | 0.38 |
| Brigatinib | ALK, RY | 0.398 | 9.4 | 5.09 | 4.31 | 40 | 0.331 | 180 | 22 | 2.49 | 8 | 3 | 2 | 0.35 |
| Cabozantinib | RET, RY | 5 | 8.3 | 5.54 | 2.76 | 37 | 0.316 | 40 | 1.99 | 4.65 | 8 | 4 | 2 | 0.31 |
| Capmatinib | MET, RY | 0.13 | 9.89 | 3.43 | 6.46 | 31 | 0.450 | 800 * | 5.29 | 2.96 | 5 | 5 | 1 | 0.49 |
| Ceritinib | ALK, RY | 0.2 | 9.7 | 6.36 | 3.34 | 38 | 0.360 | 750 | 2.22 | 3.38 | 9 | 3 | 2 | 0.28 |
| Cobimetinib | MEK1, DS | 0.79 | 9.1 | 3.78 | 5.32 | 30 | 0.428 | 60 | 42.2 | 2.73 | 4 | 2 | 2 | 0.53 |
| Crizotinib | ALK, RY | 0.63 | 9.2 | 5.04 | 4.16 | 30 | 0.432 | 500 * | 6.11 | 0.95 | 5 | 3 | 1 | 0.53 |
| Dabrafenib | B-Raf, S/T | 0.4 | 9.4 | 5.36 | 4.04 | 35 | 0.379 | 300 * | 3.27 | 5.10 | 6 | 4 | 2 | 0.37 |
| Dacomitinib | EGFR, RY | 2 | 8.7 | 5.16 | 3.54 | 33 | 0.372 | 45 | 8.74 | 3.53 | 7 | 3 | 1 | 0.47 |
| Dasatinib | BCR-Abl, NRY | 0.16 | 9.8 | 3.31 | 6.49 | 33 | 0.419 | 100 | 12.8 | 3.74 | 7 | 3 | 1 | 0.47 |
| Encorafenib | B-Raf, S/T | 0.3 | 9.52 | 3.91 | 5.61 | 36 | 0.373 | 450 | 11.2 | 2.61 | 10 | 3 | 1 | 0.37 |
| Entrectinib | TRKA, RY | 1 | 9 | 5.03 | 3.97 | 41 | 0.310 | 600 | 8.9 | 4.87 | 9 | 4 | 2 | 0.29 |
| Erdafitinib | FGFR1, RY | 2 | 8.7 | 4.18 | 4.52 | 33 | 0.372 | 8 | 13 | 1.25 | 11 | 4 | 1 | 0.41 |
| Erlotinib | EGFR, RY | 0.32 | 9.5 | 3.41 | 6.09 | 29 | 0.462 | 150 | 8.91 | 3.20 | 7 | 3 | 1 | 0.42 |
| Everolimus | FKBP12/mTOR, S/T | ? | ? | 6.2 | ? | 68 | ? | 10 | 1.63 | 7.40 | 9 | 0 | 0 | 0.13 |
| Fedratinib | JAK2, NRY | 6 | 8.22 | 4.82 | 3.40 | 37 | 0.313 | 400 | 9.49 | 3.23 | 11 | 3 | 2 | 0.35 |
| Fostamatinib | Syk, RY | 17 | 7.77 | 3.09 | 4.68 | 40 | 0.274 | 300 * | 52 | -0.52 | 10 | 3 | 1 | 0.26 |
| Gefitinib | EGFR, RY | 0.5 | 9.3 | 4.28 | 5.02 | 31 | 0.423 | 250 | 27 | 3.64 | 8 | 3 | 1 | 0.52 |
| Gilteritinib | Flt3, RY | 0.41 | 9.39 | 2.7 | 6.69 | 40 | 0.331 | 120 | 22.3 | 1.69 | 9 | 2 | 1 | 0.43 |
| Ibrutinib | BTK, NRY | 12.6 | 7.9 | 4.22 | 3.68 | 33 | 0.338 | 560 | 20.3 | 3.63 | 5 | 4 | 2 | 0.47 |
| Imatinib | BCR-Abl, NRY | 1 | 9 | 4.59 | 4.41 | 37 | 0.343 | 600 | 14.6 | 3.80 | 7 | 4 | 2 | 0.39 |
| **Infigratinib** | FGFR2, RY | 5 | 8.3 | 5.35 | 2.95 | 38 | 0.308 | 125 | 29.9 | 3.99 | 8 | 3 | 2 | 0.38 |
| Lapatinib | EGFR, RY | 1 | 9 | 6.14 | 2.86 | 40 | 0.317 | 1250 | 22.3 | 4.40 | 11 | 5 | 2 | 0.18 |
| Larotrectinib | TRK, RY | 9.7 | 8.01 | 2.95 | 5.06 | 31 | 0.364 | 200 * | 238 | 2.44 | 3 | 3 | 1 | 0.67 |
| Lenvatinib | VEGFR2, RY | 3.98 | 8.4 | 4.07 | 4.33 | 30 | 0.395 | 24 | 6.22 | 2.52 | 6 | 3 | 1 | 0.55 |
| Lorlatinib | ALK, RY | 9 | 8.05 | 2.8 | 5.25 | 30 | 0.378 | 100 | 108 | 1.62 | 0 | 3 | 1 | 0.61 |
| Midostaurin | Flt3, RY | 37 | 7.43 | 5.91 | 1.52 | 43 | 0.244 | 200 * | 15.7 | 5.43 | 3 | 6 | 1 | 0.29 |
| **Mobocertinib** | EGFR, RY | 60 | 7.22 | 5.08 | 2.14 | 43 | 0.237 | 160 | 13.6 | 3.79 | 13 | 4 | 1 | 0.17 |
| Neratinib | ErbB2/HER2, RY | 59 | 7.23 | 5.93 | 1.30 | 40 | 0.255 | 240 | 6.74 | 3.05 | 11 | 4 | 1 | 0.22 |
| Netarsudil | ROCK1/2, S/T | 1 | 9 | 4.89 | 4.11 | 34 | 0.373 | 0.01 | 0.23 | 3.42 | 8 | 4 | 2 | 0.39 |
| Nilotinib | BCR-Abl, NRY | 12.5 | 7.9 | 6.36 | 1.54 | 39 | 0.286 | 600 * | 2.01 | 5.35 | 6 | 5 | 2 | 0.27 |
| Nintedanib | FGFR, RY | 39.8 | 7.4 | 3.62 | 3.78 | 40 | 0.261 | 300 * | 30.9 | 2.57 | 8 | 4 | 2 | 0.35 |
| Osimertinib | EGFR, RY | 7 | 8.15 | 4.51 | 3.64 | 37 | 0.311 | 80 | 22.4 | 3.01 | 10 | 4 | 1 | 0.31 |
| Palbociclib | CDK4, S/T | 10 | 8 | 2.97 | 5.03 | 33 | 0.342 | 125 | 17.4 | 1.30 | 5 | 3 | 0 | 0.58 |
| Pazopanib | VEGFR2, RY | 30 | 7.52 | 3.14 | 4.38 | 31 | 0.342 | 800 | 43.3 | 3.55 | 5 | 4 | 1 | 0.49 |
| Pemigatinib | FGFR, RY | 0.5 | 9.3 | 3.66 | 5.64 | 35 | 0.375 | 13.5 | 144 | 1.80 | 6 | 3 | 1 | 0.57 |
| Pexidartinib | CSF1R, RY | 13 | 7.89 | 5.23 | 2.66 | 29 | 0.384 | 800 * | 3.15 | 4.55 | 5 | 4 | 0 | 0.47 |
| Ponatinib | BCR-Abl, NRY | 1 | 9 | 4.46 | 4.54 | 39 | 0.325 | 45 | 2.95 | 4.54 | 8 | 4 | 2 | 0.39 |
| Pralsetinib | RET, RY | 0.5 | 9.3 | 4.2 | 5.10 | 39 | 0.336 | 400 | 10.1 | 3.64 | 6 | 4 | 0 | 0.31 |
| Regorafenib | VEGFR2, RY | 4.2 | 8.4 | 5.69 | 2.71 | 33 | 0.359 | 160 | 1.02 | 4.49 | 5 | 3 | 2 | 0.41 |
| Ribociclib | CDK4, S/T | 10 | 8 | 2.8 | 5.20 | 32 | 0.353 | 600 | 231 | 0.91 | 5 | 3 | 1 | 0.64 |
| Ripretinib | Kit, RY | 3 | 8.52 | 5.67 | 2.85 | 33 | 0.364 | 150 | 5.83 | 4.38 | 5 | 4 | 2 | 0.32 |
| Ruxolitinib | JAK1, NRY | 1.2 | 8.92 | 3.47 | 5.45 | 23 | 0.547 | 20 * | 116 | 2.48 | 4 | 3 | 0 | 0.8 |
| Selpercatinib | RET, RY | 1 | 9 | 3.28 | 5.72 | 39 | 0.325 | 320 * | 29.9 | 3.11 | 8 | 4 | 0 | 0.37 |
| Selumetinib | MEK1, DS | 14 | 7.85 | 3.53 | 4.32 | 27 | 0.410 | 80 * | 21 | 4.27 | 6 | 3 | 1 | 0.39 |
| Sirolimus | FKBP12/mTOR, S/T | ? | ? | 6.18 | ? | 65 | ? | 2 | 1.73 | 7.45 | 6 | 0 | 0 | 0.16 |
| Sorafenib | VEGFR1, RY | 15.8 | 7.8 | 5.55 | 2.25 | 32 | 0.344 | 800 * | 1.71 | 4.34 | 5 | 3 | 2 | 0.46 |
| Sunitinib | VEGFR2, RY | 3.98 | 8.4 | 3.33 | 5.07 | 29 | 0.408 | 50 | 30.8 | 1.28 | 7 | 2 | 0 | 0.63 |
| Temsirolimus | FKBP12/mTOR, S/T | ? | ? | 4.39 | ? | 73 | ? | 25 * * | 2.35 | ? | 7 | 0 | 0 | ? |
| **Tepotinib** | MET, RY | 1 | 9 | 4.01 | 4.99 | 37 | 0.343 | 450 | ? | 2.26 | 6 | 4 | 2 | 0.38 |
| **Tivozanib** | VEGFR2, RY | 6.5 | 8.19 | 5.64 | 2.55 | 37 | 0.312 | 1.34 | 52.1 | 4.16 | 11 | 4 | 1 | 0.39 |
| Tofacitinib | JAK1, NRY | 0.79 | 9.1 | 1.54 | 7.56 | 23 | 0.558 | 10 * | 299 | 1.19 | 3 | 2 | 0 | 0.93 |
| Trametinib | MEK1, DS | 3.4 | 8.47 | 3.94 | 4.53 | 37 | 0.323 | 2 | 30.7 | 3.18 | 5 | 3 | 2 | 0.33 |
| **Trilaciclib** | CDK4/6, S/T | 1 | 9 | 2.72 | 6.28 | 33 | 0.385 | 480 | 260 | 2.29 | 3 | 3 | 0 | 0.64 |
| Tucatinib | ErbB2/HER2, RY | 8 | 8.1 | 5.09 | 3.01 | 36 | 0.317 | 600 * | 4 | 5.25 | 6 | 5 | 1 | 0.36 |
| Upadacitinib | JAK1, NRY | 43 | 7.37 | 2.91 | 4.46 | 27 | 0.385 | 15 | 70.7 | 0.85 | 3 | 3 | 0 | 0.73 |
| Vandetanib | RET, RY | 50 | 7.3 | 5 | 2.30 | 30 | 0.343 | 300 | 10.2 | 2.81 | 6 | 3 | 1 | 0.54 |
| Vemurafenib | B-Raf, S/T | 3.98 | 8.4 | 5.54 | 2.86 | 33 | 0.359 | 1920 * | 0.36 | 4.61 | 7 | 4 | 2 | 0.33 |
| Zanubrutinib | BTK, NRY | 0.3 | 9.52 | 4.22 | 5.30 | 35 | 0.384 | 320 * | 10.3 | 3.42 | 6 | 3 | 2 | 0.52 |

[a] Drugs previously not reviewed (Refs. [10–12]) are given in **bold** type.
[b] NRY, non-receptor protein-tyrosine kinase; RY, receptor protein-tyrosine kinase; S/T, protein-serine/threonine kinase; DS; dual specificity protein kinase (catalyzes protein-tyrosine/threonine/serine phosphorylation but evolutionarily in the protein-serine/threonine kinase family).

[c] Representative values obtained from www.ebi.ac.ug/chembl/ and from klifs.net.
[d] Values for atom-based ALogP from https://www.ebi.ac.uk/chembl/
[e] LipE = $p$IC$_{50}$ – ALogP
[f] N, Number of heavy atoms.
[g] LE = – 2.303 RT Log$_{10}$ $K_i$/N where N is the number of heavy (non-hydrogen) atoms in the drug.
[h] Dosage from FDA label; * , one-half of total daily dose taken twice per day; * *, once weekly.
[i] Values from https://go.drugbank.com/drugs/
[j] nRb, number of Rotatable bonds.
[k] nAr, number of Aromatic rings.
[l] QED, summed, weighted desirability (scores using MW + ALogP + HBD + HBA + PSA + nRotB + nAr) obtained from https://www.ebi.ac.uk/chembl/; see Ref. [92] for a full explanation.

algorithm [94,95]. It is based upon the identity and number of the constituent atoms, the bonding pattern, and the nature of the chemical bonds (single, double, triple, aromatic). The molecular complexity ranges from 0 for simple ions to several thousand for complicated natural products. Larger compounds usually possess a higher molecular complexity value than smaller ones. Contrariwise, compounds containing few distinct elements and those that are highly symmetrical possess a lower molecular complexity value. The molecular complexity values for the medicines in this review were acquired from PubChem (https://pubchem.ncbi.nlm.nih.gov/). For all of the FDA-approved drugs, the mean complexity value is 776 with a range from 453 (ruxolitinib) to 2010 (temsirolimus). As expected, the large macrolide agents exhibit the greatest molecular complexity values. There are no recommended or optimal molecular complexity values for orally bioavailable medicines; however, this property may be helpful in determining the ease or difficulty of drug production, an important consideration in the commercial synthesis of pharmaceutical agents.

Leeson et al. compared drug properties during different eras including 1990–2009 and 2010–2020 [92]. They reported that the molecular weight and lipophilicity of approved drugs have increased with time. We compared the averages of selected properties of FDA-approved protein kinase antagonists during two time frames: 2001 – 2011 and 2012 – 2021. This analysis excluded the three large macrolides. The average molecular weight increased from 458 to 488 during this period as well as the heavy atom count (32.1–34.8), the polar surface area (93.0–99.3 Å$^2$), and molecular complexity (650−744). The mean ALogP decreased (3.97–3.60) and the lipophilic efficiency increased slightly (4.88–5.00) in favorable directions. In contrast, the ligand efficiency decreased (0.399–0.353) in an unfavorable direction. However, the average number of hydrogen bond donors and acceptors, the number of rotatable bonds, the ring count, and the potency ($K_i$ values) were essentially unchanged (Table 10). Leeson et al. reported that the molecular weight of all approved drugs, including protein kinase antagonists, has increased over time [92].

Ritchie and Macdonald reviewed the use of aromaticity in the drug discovery process [96]. Aromaticity describes cyclically conjugated molecules with a stability owing to electron delocalization that is significantly greater than a localized Kekulé structure. They considered bicyclic and tricyclic structures as containing two and three aromatic rings, respectively. Aromatic ring counts encompass both carbon and heteroatom components. The effect of increasing carboaromatic rings had a detrimental effect on pharmacologic efficacy by decreasing aqueous solubility, inhibiting CYP450, and increasing binding to serum albumin. We find that the average number of aromatic rings in the 68-approved protein kinase antagonists was 3.37 and the mean number of benzene moieties was 1.10. All of the drugs with the exception of the three macrolides have a least two aromatic rings; midostaurin had the largest number of rings at six. Fifteen of the drugs lacked benzene fragments and the number of drugs possessing one or two benzenes was about evenly distributed among the remainder (Table 9).

Bayliss et al. evaluated the dose, solubility, and lipophilicity for oral drug and oral drug candidates [97]. They summarized work suggesting that doses of less than 100 mg daily can reduce the risk of toxicity. The range of dosages for protein kinase antagonists given orally is from 1.34 mg to 1920 mg daily with an average of 312 mg. The daily doses range from 1.34, 2, and 2 mg for tivozanib, trametinib, and baricitinib and 1200, 1250, and 1920 mg for alectinib, lapatinib, and vemurafenib, respectively. Only 24 have doses of 100 mg or less. Bayliss et al. suggested that drugs with a solubility of less than 100 μg/ml are associated with increased risk of failure during drug development [97]. We tabulated the aqueous solubility of the approved protein kinase inhibitors and found a range from 0.36 μg/ml (vemurafenib) to 357 μg/ml (tepotinib) with a mean value of 36.1 μg/ml. The range in dosages and solubilities among the FDA-approved drugs is nearly three orders of magnitude.

## 7. Epilogue and perspective

Although substantial progress has been made in the development and discovery of small molecule protein kinase antagonists since the FDA-approval of imatinib in 2001, this field remains in its early stages. The increased expression of many protein kinases in primary human tumors are understudied enzymes that may have important functions during tumorigenesis [98]. Moreover, these understudied enzymes may have therapeutic utility. Examples include cyclin-dependent protein kinase 12 (CDK12), mitogen-activated protein kinase kinase kinase 1 (MAP3K1), and eukaryotic elongation factor 2 kinase (EEF2K). Most of the FDA-approved kinase inhibitors are antineoplastic and others are

**Table 10**
Comparison of the averages of selected properties of FDA-approved protein kinase inhibitors in two time frames.

| Year | No. of drugs | MW, Da | Heavy atoms | HD[b] | HA[c] | ALogP[a,d] | Rotatable bonds | PSA[e], Å$^2$ | Ring count[f] | Complexity[g] | $K_i$, nM | p$K_i$ | LipE | LE |
|---|---|---|---|---|---|---|---|---|---|---|---|---|---|---|
| 2001–2011 | 13 | 458 | 32.1 | 1.92 | 7.00 | 3.97 | 6.79 | 93.0 | 4.00 | 650 | 9.31 | 8.62 | 4.88 | 0.399 |
| 2012–2021 | 52 | 488 | 34.8 | 2.13 | 7.33 | 3.60 | 6.45 | 99.3 | 4.45 | 744 | 9.62 | 8.55 | 5.00 | 0.353 |
| 2001–2021 | 65 | 482 | 34.2 | 2.09 | 7.26 | 3.67 | 6.52 | 98.0 | 4.35 | 723 | 9.56 | 8.56 | 4.97 | 0.362 |

[a] All data from NIH PubChem except for ALogP, which was obtained from https://www.ebi.ac.uk/chembl/.
[b] No. of hydrogen bond donors.
[c] No. of hydrogen bond acceptors.
[d] Atom-based calculated Log of the partition coefficient.
[e] PSA, polar surface area.
[f] Aromatic and nonaromatic.
[g] Values obtained from https://pubchem.ncbi.nlm.nih.gov/.

immunomodulators [10,99–101]. Because of the inherent genetic changes of neoplastic cells, resistance to protein kinase antagonists occurs on a nearly universal basis. Such resistance has led to the fabrication and development of second, third, and later generation inhibitors that target the same enzyme and disease. Moreover, acquired drug resistance is frequently the result of gatekeeper mutations in the original protein kinase target [3]. The T790M gatekeeper mutation in EGFR is a case in point and the third most frequently observed protein kinase mutation that is responsible for about half of all examples of acquired EGFR inhibitor resistance. Although inflammatory processes per se are not associated with genetic instability, it is unclear whether acquired resistance occurs during the treatment of inflammatory disorders.

Owing to the 244 protein kinases that map to disease loci or cancer amplicons [8], it is likely that (i) a significant increase in the number of drugs inhibiting additional protein kinases will occur and (ii) new medicines will be discovered for the treatment of many more illnesses [102,103]. Adding new protein kinases to the therapeutic armamentarium will require the identification of the signaling pathways and networks – besides the RAS-Raf-MEK MAP kinase and phosphatidylinositol 3-kinase-AKT signaling modules [104] – in addition to upstream activating factors that contribute to the pathogenesis of currently untargeted illnesses. Along with the 68 approved protein kinase inhibitors considered in this paper, the FDA has approved five drugs that inhibit phosphatidylinositol 3-kinases, lipid kinases that are members of the atypical protein kinase family [9]. These include alpelisib – an orally effective PI 3-kinase-α inhibitor that is used for the treatment of breast cancer – and copanlisib, duvelisib, idelalisib, and umbralisib that are PI 3-kinase-δ inhibitors that are approved for the third-line treatment of follicular lymphomas and other hematological disorders. As the protein kinase inhibitor discipline develops during the next decades, it is likely that protein kinase inhibitors with new pharmacophores, scaffolds, and chemotypes will be created [105]. There are only four FDA-approved type III allosteric inhibitors (trametinib, selumetinib, cobimetinib, and binimetinib) and these block the action of MEK1/2. One can anticipate that additional allosteric inhibitors will be created that are directed toward novel enzymes that are part of a variety of protein kinase signal transduction modules [106]. Furthermore, it is likely that new irreversible inhibitors that target protein kinases with –SH groups near the ATP-binding site such as mobocertinib will be forthcoming.

## Conflict of interest

The author is unaware of any affiliations, memberships, or financial holdings that might be perceived as affecting the objectivity of this review.

## Acknowledgments

I thank Dr. Albert J. Kooistra for providing the template depicted in Fig. 3 and Laura M. Roskoski for providing editorial and bibliographic assistance. I also thank Jasper Martinsek and Josie Rudnicki for their help in preparing the figures and W.S. Sheppard and Pasha Brezina for their help in structural analyses. The colored figures in this paper were evaluated to ensure that their perception was accurately conveyed to colorblind readers [107].

## Appendix A. Supporting information

Supplementary data associated with this article can be found in the online version at doi:10.1016/j.phrs.2021.106037.

## References

[1] P. Cohen, Protein kinases – the major drug targets of the twenty-first century? Nat. Rev. Drug Discov. 1 (2002) 309–315, https://doi.org/10.1038/nrd773.
[2] R. Roskoski Jr., A historical overview of protein kinases and their targeted small molecule inhibitors, Pharm. Res. 100 (2015) 1–23, https://doi.org/10.1016/j.phrs.2015.07.010.
[3] P. Cohen, D. Cross, P.A. Jänne, Kinase drug discovery 20 years after imatinib: progress and future directions, Nat. Rev. Drug Discov. 20 (2021) 551–569, https://doi.org/10.1038/s41573-021-00195-4.
[4] M.M. Attwood, D. Fabbro, A.V. Sokolov, S. Knapp, H.B. Schiöth, Trends in kinase drug discovery: targets, indications and inhibitor design, Nat. Rev. Drug Discov. 20 (2021) 839–861.
[5] G.K. Kanev, C. de Graaf, I.J.P. de Esch, R. Leurs, T. Würdinger, B.A. Westerman, A.J. Kooistra, The landscape of atypical and eukaryotic protein kinases, Trends Pharm. Sci. 40 (2019) 818–832, https://doi.org/10.1016/j.tips.2019.09.002.
[6] F. Carles, S. Bourg, C. Meyer, P. Bonnet, PKIDB: a curated, annotated and updated database of protein kinase inhibitors in clinical trials, Molecules (2018) 23, https://doi.org/10.3390/molecules23040908.
[7] P.M. Fischer, Approved and experimental small-molecule oncology kinase inhibitor drugs: a mid-2016 overview, Med Res. Rev. 37 (2017) 314–367, https://doi.org/10.1002/med.21409.
[8] G. Manning, D.B. Whyte, R. Martinez, T. Hunter, S. Sudarsanam, The protein kinase complement of the human genome, Science 298 (2002) 1912–1934, https://doi.org/10.1126/science.1075762.
[9] R. Roskoski Jr., Properties of FDA-approved small molecule phosphatidylinositol 3-kinase inhibitors prescribed for the treatment of malignancies, Pharm. Res. 168 (2021), 105579, https://doi.org/10.1016/j.phrs.2021.105579.
[10] R. Roskoski Jr., Properties of FDA-approved small molecule protein kinase inhibitors, Pharm. Res. 144 (2019) 19–50, https://doi.org/10.1016/j.phrs.2019.03.006.
[11] R. Roskoski Jr., Properties of FDA-approved small molecule protein kinase inhibitors: a 2020 update, Pharm. Res. 152 (2020), 104609, https://doi.org/10.1016/j.phrs.2019.104609.
[12] R. Roskoski Jr., Properties of FDA-approved small molecule protein kinase inhibitors: a 2021 update, Pharm. Res. 165 (2021), 105463, https://doi.org/10.1016/j.phrs.2021.105463.
[13] S.H. Myers, V.G. Brunton, A. Unciti-Broceta, AXL inhibitors in cancer: a medicinal chemistry perspective, J. Med. Chem. 59 (2016) 3593–3608, https://doi.org/10.1021/acs.jmedchem.5b01273.
[14] B.L. Roth, D.J. Sheffler, W.K. Kroeze, Magic shotguns versus magic bullets: selectively non-selective drugs for mood disorders and schizophrenia, Nat. Rev. Drug Discov. 3 (2004) 353–359, https://doi.org/10.1038/nrd1346.
[15] R. Roskoski Jr., Orally effective FDA-approved protein kinase targeted covalent inhibitors (TCIs), Pharm. Res. 165 (2021), 105422, https://doi.org/10.1016/j.phrs.2021.105422.
[16] D.R. Knighton, J.H. Zheng, L.F. Ten Eyck, V.A. Ashford, N.H. Xuong, S.S. Taylor, J.M. Sowadski, Crystal structure of the catalytic subunit of cyclic adenosine monophosphate-dependent protein kinase, Science 253 (1991) 407–414, https://doi.org/10.1126/science.1862342.
[17] A.P. Kornev, S.S. Taylor, Dynamics-driven allostery in protein kinases, Trends Biochem Sci. 40 (2015) 628–647, https://doi.org/10.1016/j.tibs.2015.09.002.
[18] S.S. Taylor, J. Wu, J.G.H. Bruystens, J.C. Del Rio, T.W. Lu, A.P. Kornev, L.F. Ten Eyck, From structure to the dynamic regulation of a molecular switch: a journey over 3 decades, J. Biol. Chem. 296 (2021), 100746, https://doi.org/10.1016/j.jbc.2021.100746.
[19] R. Roskoski Jr., Cyclin-dependent protein serine/threonine kinase inhibitors as anticancer drugs, Pharm. Res. 139 (2019) 471–488, https://doi.org/10.1016/j.phrs.2018.11.035.
[20] R. Roskoski Jr., Hydrophobic and polar interactions of FDA-approved small molecule protein kinase inhibitors with their target enzymes, Pharm. Res. 169 (2021), 105660, https://doi.org/10.1016/j.phrs.2021.105660.
[21] S.K. Hanks, T. Hunter, Protein kinases 6. The eukaryotic protein kinase superfamily: kinase (catalytic) domain structure and classification, FASEB J. 9 (1995) 576–596.
[22] E.A. Madhusudan, Trafny, N.H. Xuong, J.A. Adams, L.F. Ten Eyck, S.S. Taylor, J. M. Sowadski, cAMP-dependent protein kinase: crystallographic insights into substrate recognition and phosphotransfer, Protein Sci. 3 (1994) 176–187, https://doi.org/10.1002/pro.5560030203.
[23] J. Zhou, J.A. Adams, Participation of ADP dissociation in the rate-determining step in cAMP-dependent protein kinase, Biochemistry 36 (1997) 15733–15738, https://doi.org/10.1021/bi971438n.
[24] P.A. Schwartz, B.W. Murray, Protein kinase biochemistry and drug discovery, Bioorg. Chem. 39 (2011) 192–210, https://doi.org/10.1016/j.bioorg.2011.07.004.
[25] A.P. Kornev, S.S. Taylor, Defining the conserved internal architecture of a protein kinase, Biochim Biophys. Acta 1804 (2010) 440–444, https://doi.org/10.1016/j.bbapap.2009.10.017.
[26] V. Modi, R.L. Dunbrack Jr., Defining a new nomenclature for the structures of active and inactive kinases, Proc. Natl. Acad. Sci. USA 116 (2019) 6818–6827, https://doi.org/10.1073/pnas.1814279116.
[27] V. Modi, R.L. Dunbrack, Kincore: a web resource for structural classification of protein kinases and their inhibitors, Nucleic Acids Res. (2021) gkab920, https://doi.org/10.1093/nar/gkab920.
[28] A.P. Kornev, N.M. Haste, S.S. Taylor, L.F. Ten Eyck, Surface comparison of active and inactive protein kinases identifies a conserved activation mechanism, Proc. Natl. Acad. Sci. USA 103 (2006) 17783–17788, https://doi.org/10.1073/pnas.0607656103.

[29] A.P. Kornev, S.S. Taylor, L.F. Ten Eyck, A helix scaffold for the assembly of active protein kinases, Proc. Natl. Acad. Sci. USA 105 (2008) 14377–14382, https://doi.org/10.1073/pnas.0807988105.
[30] H.S. Meharena, P. Chang, M.M. Keshwani, K. Oruganty, A.K. Nene, N. Kannan, S. S. Taylor, A.P. Kornev, Deciphering the structural basis of eukaryotic protein kinase regulation, PLoS Biol. 11 (2013), e1001690, https://doi.org/10.1371/journal.pbio.1001680.
[31] R. Roskoski Jr., Classification of small molecule protein kinase inhibitors based upon the structures of their drug-enzyme complexes, Pharm. Res. 103 (2016) 26–48, https://doi.org/10.1016/j.phrs.2015.10.021.
[32] R. Roskoski Jr., The ErbB/HER family of protein-tyrosine kinases and cancer, Pharm. Res. 79 (2014) 34–74, https://doi.org/10.1016/j.phrs.2013.11.002.
[33] R. Roskoski Jr., ErbB/HER protein-tyrosine kinases: Structure and small molecule inhibitors, Pharm. Res. 87 (2014) 42–59, https://doi.org/10.1016/j.phrs.2014.06.001.
[34] R. Roskoski Jr., Small molecule inhibitors targeting the EGFR/ErbB family of protein-tyrosine kinases in human cancers, Pharm. Res. 139 (2019) 395–411, https://doi.org/10.1016/j.phrs.2018.11.014.
[35] R. Roskoski Jr., Anaplastic lymphoma kinase (ALK): structure, oncogenic activation, and pharmacological inhibition, Pharm. Res. 68 (2013) 68–94, https://doi.org/10.1016/j.phrs.2012.11.007.
[36] R. Roskoski Jr., Anaplastic lymphoma kinase (ALK) inhibitors in the treatment of ALK-driven lung cancers, Pharm. Res. 117 (2017) 343–356, https://doi.org/10.1016/j.phrs.2017.01.007.
[37] R. Roskoski Jr., The preclinical profile of crizotinib in the treatment of non-small cell lung cancer and other neoplastic disorders, Expert Opin. Drug Dis. 8 (2013) 1165–1179, https://doi.org/10.1517/17460441.2013.813015.
[38] R. Roskoski Jr., The role of fibroblast growth factor receptor (FGFR) protein-tyrosine kinase inhibitors in the treatment of cancers including those of the urinary bladder, Pharm. Res. 151 (2020), 104567, https://doi.org/10.1016/j.phrs.2019.104567.
[39] R. Roskoski Jr., The role of small molecule platelet-derived growth factor receptor (PDGFR) inhibitors in the treatment of neoplastic disorders, Pharm. Res. 129 (2018) 65–83, https://doi.org/10.1016/j.phrs.2018.01.021.
[40] R. Roskoski Jr., The role of small molecule Kit protein-tyrosine kinase inhibitors in the treatment of neoplastic disorders, Pharm. Res. 133 (2018) 35–52, https://doi.org/10.1016/j.phrs.2018.04.020.
[41] R. Roskoski Jr., Vascular endothelial growth factor (VEGF) and VEGF receptor inhibitors in the treatment of renal cell carcinomas, Pharm. Res. 120 (2017) 116–132, https://doi.org/10.1016/j.phrs.2017.03.010.
[42] R. Roskoski Jr., A. Sadeghi-Nejad, Role of RET protein-tyrosine kinase inhibitors in the treatment RET-driven thyroid and lung cancers, Pharm. Res. 128 (2018) 1–17, https://doi.org/10.1016/j.phrs.2017.12.021.
[43] R. Roskoski Jr., The role of small molecule Flt3 receptor protein-tyrosine kinase inhibitors in the treatment of Flt3-positive acute myelogenous leukemias, Pharm. Res. 155 (2020), 104725, https://doi.org/10.1016/j.phrs.2020.104725.
[44] R. Roskoski Jr., ROS1 protein-tyrosine kinase inhibitors in the treatment of ROS1 fusion protein-driven non-small cell lung cancers, Pharm. Res. 121 (2017) 202–212, https://doi.org/10.1016/j.phrs.2017.04.022.
[45] R. Roskoski Jr., Src protein-tyrosine kinase structure, mechanism, and small molecule inhibitors, Pharm. Res. 94 (2015) 9–25, https://doi.org/10.1016/j.phrs.2015.01.003.
[46] M.C. Frame, R. Roskoski Jr., Src family tyrosine kinases. Reference Module in Life Sciences, Elsevier, Amsterdam, 2017, pp. 1–11, https://doi.org/10.1016/B978-0-12-809633-8.07199-5.
[47] R. Roskoski Jr., Ibrutinib inhibition of Bruton protein-tyrosine kinase (BTK) in the treatment of B cell neoplasms, Pharm. Res. 113 (2016) 395–408, https://doi.org/10.1016/j.phrs.2016.09.011.
[48] R. Roskoski Jr., Janus kinase (JAK) inhibitors in the treatment of inflammatory and neoplastic diseases, Pharm. Res. 111 (2016) 784–803, https://doi.org/10.1016/j.phrs.2016.07.038.
[49] R. Roskoski Jr., MEK1/2 dual-specificity protein kinases: structure and regulation, Biochem Biophys. Res. Commun. 417 (2012) 5–10, https://doi.org/10.1016/j.bbrc.2011.11.145.
[50] R. Roskoski Jr., Allosteric MEK1/2 inhibitors including cobimetanib and trametinib in the treatment of cutaneous melanomas, Pharm. Res. 117 (2017) 20–31, https://doi.org/10.1016/j.phrs.2016.12.009.
[51] R. Roskoski Jr., Targeting oncogenic Raf protein-serine/threonine kinases in human cancers, Pharm. Res. 135 (2018) 239–258, https://doi.org/10.1016/j.phrs.2018.08.013.
[52] R. Roskoski Jr., RAF protein-serine/threonine kinases: structure and regulation, Biochem Biophys. Res. Commun. 399 (2010) 313–317, https://doi.org/10.1016/j.bbrc.2010.07.092.
[53] R. Roskoski Jr., ERK1/2 MAP kinases: structure, function, and regulation, Pharm. Res. 66 (2012) 105–143, https://doi.org/10.1016/j.phrs.2012.04.005.
[54] R. Roskoski Jr., Targeting ERK1/2 protein-serine/threonine kinases in human cancers, Pharm. Res. 142 (2019) 151–168, https://doi.org/10.1016/j.phrs.2019.01.039.
[55] R. Roskoski Jr., Cyclin-dependent protein kinase inhibitors including palbociclib as anticancer drugs, Pharm. Res. 107 (2016) 249–275, https://doi.org/10.1016/j.phrs.2016.03.012.
[56] Y. Liu, K. Shah, F. Yang, L. Witucki, K.M. Shokat, A molecular gate which controls unnatural ATP analogue recognition by the tyrosine kinase v-Src, Bioorg. Med Chem. 6 (1998) 1219–1226, https://doi.org/10.1016/s0968-0896(98)00099-6.
[57] A.C. Dar, K.M. Shokat, The evolution of protein kinase inhibitors from antagonists to agonists of cellular signaling, Annu Rev. Biochem. 80 (2011) 769–795, https://doi.org/10.1146/annurev-biochem-090308-173656.
[58] P.M. Ung, R. Rahman, A. Schlessinger, Redefining the protein kinase conformational space with machine learning, Cell Chem. Biol. 25 (2018) 916–924, https://doi.org/10.1016/j.chembiol.2018.05.002.
[59] R. Hu, H. Xu, P. Jia, Z. Zhao, KinaseMD: kinase mutations and drug response database, Nucleic Acids Res. 49 (D1) (2021) D552–D561, https://doi.org/10.1093/nar/gkaa945.
[60] F. Zuccotto, E. Ardini, E. Casale, M. Angiolini, Through the "gatekeeper door": exploiting the active kinase conformation, J. Med. Chem. 53 (2010) 2691–2694, https://doi.org/10.1021/jm901443h.
[61] L.K. Gavrin, E. Saiah, Approaches to discover non-ATP site inhibitors, Med Chem. Commun. 4 (2013) 41.
[62] V. Lamba, I. Ghosh, New directions in targeting protein kinases: focusing upon true allosteric and bivalent inhibitors, Curr. Pharm. Des. 18 (2012) 2936–2945, https://doi.org/10.2174/138161212800672813.
[63] J.J. Liao, Molecular recognition of protein kinase binding pockets for design of potent and selective kinase inhibitors, J. Med Chem. 50 (2007) 409–424, https://doi.org/10.1021/jm0608107.
[64] O.P. van Linden, A.J. Kooistra, R. Leurs, I.J. de Esch, C. de Graaf, KLIFS: a knowledge-based structural database to navigate kinase-ligand interaction space, J. Med. Chem. 57 (2014) 249–277, https://doi.org/10.1021/jm400378w.
[65] A.J. Kooistra, G.K. Kanev, O.P. van Linden, R. Leurs, I.J. de Esch, C. de Graaf, KLIFS: a structural kinase-ligand interaction database, Nucleic Acids Res. 44 (D1) (2016) D365–D371, https://doi.org/10.1093/nar/gkv1082.
[66] G.K. Kanev, C. de Graaf, B.A. Westerman, I.J.P. de Esch, A.J. Kooistra, KLIFS: an overhaul after the first 5 years of supporting kinase research, Nucleic Acids Res. (2020) gkaa895, https://doi.org/10.1093/nar/gkaa895.
[67] B. Wienen-Schmidt, D. Schmidt, H.D. Gerber, A. Heine, H. Gohlke, G. Klebe, Surprising non-additivity of methyl groups in drug-kinase interaction, ACS Chem. Biol. 14 (2019) 2585–2594, https://doi.org/10.1021/acschembio.9b00476.
[68] D. Bajusz, G.G. Ferenczy, G.M. Keserű, Structure-based virtual screening approaches in kinase-directed drug discovery, Curr. Top. Med. Chem. 17 (2017) 2235–2259, https://doi.org/10.2174/1568026617666170224121313.
[69] P. Wu, T.E. Nielsen, M.H. Clausen, FDA-approved small-molecule kinase inhibitors, Trends Pharm. Sci. 36 (2015) 422–439, https://doi.org/10.1016/j.tips.2015.04.005.
[70] V. Guagnano, P. Furet, C. Spanka, V. Bordas, M. Le Douget, C. Stamm, J. Brueggen, M.R. Jensen, C. Schnell, H. Schmid, M. Wartmann, J. Berghausen, P. Drueckes, A. Zimmerlin, D. Bussiere, J. Murray, D. Graus Porta, Discovery of 3-(2,6-dichloro-3,5-dimethoxy-phenyl)-1-{6-[4-(4-ethyl-piperazin-1-yl)-phenylamino]-pyrimidin-4-yl}-1-methyl-urea (NVP-BGJ398), a potent and selective inhibitor of the fibroblast growth factor receptor family of receptor tyrosine kinase, J. Med. Chem. 54 (2011) 7066–7083, https://doi.org/10.1021/jm2006222.
[71] J. Yu, A. Mahipal, R. Kim, Targeted therapy for advanced or metastatic cholangiocarcinoma: focus on the clinical potential of infigratinib, Onco Targets Ther. 14 (2021) 5145–5160, https://doi.org/10.2147/OTT.S272208.
[72] P.K. Paik, E. Felip, R. Veillon, H. Sakai, A.B. Cortot, M.C. Garassino, J. Mazieres, S. Viteri, H. Senellart, J. Van Meerbeeck, J. Raskin, N. Reinmuth, P. Conte, D. Kowalski, B.C. Cho, J.D. Patel, L. Horn, F. Griesinger, J.Y. Han, Y.C. Kim, G. C. Chang, C.L. Tsai, J.C. Yang, Y.M. Chen, E.F. Smit, A.J. van der Wekken, T. Kato, D. Juraeva, C. Stroh, R. Bruns, J. Straub, A. Johne, J. Scheele, J.V. Heymach, X. Le, Tepotinib in non-small-cell lung cancer with *MET* exon 14 skipping mutations, New Engl. J. Med. 383 (2020) 931–943, https://doi.org/10.1056/NEJMoa2004407.
[73] L.N. Mathieu, E. Larkins, O. Akinboro, P. Roy, A.K. Amatya, M.H. Fiero, P. S. Mishra-Kalyani, W.S. Helms, C.E. Myers, A.M. Skinner, S. Aungst, R. Jin, H. Zhao, H. Xia, J.F. Zirkelbach, Y. Bi, Y. Li, J. Liu, M. Grimstein, X. Zhang, S. Woods, K. Reece, A.M. Abukhdeir, S. Ghosh, R. Philip, S. Tang, K.B. Goldberg, R. Pazdur, J.A. Beaver, H. Singh, FDA approval summary: capmatinib and tepotinib for the treatment of metastatic NSCLC harboring MET exon 14 skipping mutations or alterations, Clin. Cancer Res. (2021), https://doi.org/10.1158/1078-0432.CCR-21-1566.
[74] K. Nakamura, E. Taguchi, T. Miura, A. Yamamoto, K. Takahashi, F. Bichat, N. Guilbaud, K. Hasegawa, K. Kubo, Y. Fujiwara, R. Suzuki, K. Kubo, M. Shibuya, T. Isae, KRN951, a highly potent inhibitor of vascular endothelial growth factor receptor tyrosine kinases, has antitumor activities and affects functional vascular properties, Cancer Res. 66 (2006) 9134–9142, https://doi.org/10.1158/0008-5472.CAN-05-4290.
[75] E. Chang, C. Weinstock, L. Zhang, M.H. Fiero, M. Zhao, E. Zahalka, T.K. Ricks, J. Fourie Zirkelbach, J. Qiu, J. Yu, X.H. Chen, V. Bhatnagar, K.B. Goldberg, S. Tang, P.G. Kluetz, R. Pazdur, A. Ibrahim, J.A. Beaver, L. Amiri-Kordestani, FDA approval summary: tivozanib for relapsed or refractory renal cell carcinoma, Clin. Cancer Res. (2021), https://doi.org/10.1158/1078-0432.CCR-21-2334.
[76] H.A. Blair, Belumosudil: first approval, Drugs 81 (2021) 1677–1682, https://doi.org/10.1007/s40265-021-01593-z.
[77] C.S. Cutler, S.J. Lee, S. Arai, M. Rotta, B. Zoghi, A. Lazaryan, A. Ramakrishnan, Z. DeFilipp, A. Salhotra, W. Chai-Ho, R.S. Mehta, T. Wang, M. Arora, I. Pusic, A. Saad, N.N. Shah, S. Abhyankar, C. Bachier, J.P. Galvin, A. Im, A. Langston, J. L. Liesveld, M. Juckett, A. Logan, L. Schachter, A. Alavi, D.S. Howard, H. Waksal, J. Ryan, D. Eiznhamer, S.K. Aggarwal, J. Ieyoub, O. Schueller, L.S. Green, Z. Yang, H. Krenz, M. Jagasia, B.R. Blazar, S.Z. Pavletic, Belumosudil for chronic graft-versus-host disease (cGVHD) after 2 or more prior lines of therapy: the

ROCKstar study, Blood (2021), 2021012021, https://doi.org/10.1182/blood.2021012021.
[78] A. Zanin-Zhorov, B.R. Blazar, ROCK2, a critical regulator of immune modulation and fibrosis has emerged as a therapeutic target in chronic graft-versus-host disease, Clin. Immunol. 230 (2021), 108823, https://doi.org/10.1016/j.clim.2021.108823.
[79] M. Jagasia, A. Lazaryan, C.R. Bachier, A. Salhotra, D.J. Weisdorf, B. Zoghi, J. Essell, L. Green, O. Schueller, J. Patel, A. Zanin-Zhorov, J.M. Weiss, Z. Yang, D. Eiznhamer, S.K. Aggarwal, B.R. Blazar, S.J. Lee, ROCK2 inhibition with belumosudil (KD025) for the treatment of chronic graft-versus-host disease, J. Clin. Oncol. 39 (2021) 1888–1898, https://doi.org/10.1200/JCO.20.02754.
[80] F. Gonzalvez, S. Vincent, T.E. Baker, A.E. Gould, S. Li, S.D. Wardwell, S. Nadworny, Y. Ning, S. Zhang, W.S. Huang, Y. Hu, F. Li, M.T. Greenfield, S. G. Zech, B. Das, N.I. Narasimhan, T. Clackson, D. Dalgarno, W.C. Shakespeare, M. Fitzgerald, J. Chouitar, R.J. Griffin, S. Liu, K.K. Wong, X. Zhu, V.M. Rivera, Mobocertinib (TAK-788): a targeted inhibitor of *EGFR* exon 20 insertion mutants in non-small cell lung cancer, Cancer Discov. 11 (2021) 1672–1687, https://doi.org/10.1158/2159-8290.CD-20-1683.
[81] G.J. Riely, J.W. Neal, D.R. Camidge, A.I. Spira, Z. Piotrowska, D.B. Costa, A. S. Tsao, J.D. Patel, S.M. Gadgeel, L. Bazhenova, V.W. Zhu, H.L. West, T. Mekhail, R.D. Gentzler, D. Nguyen, S. Vincent, S. Zhang, J. Lin, V. Bunn, S. Jin, S. Li, P. A. Jänne, Activity and safety of mobocertinib (TAK-788) in previously treated non-small cell lung cancer with *EGFR* exon 20 insertion mutations from a phase I/II trial, Cancer Discov. 11 (2021) 1688–1699, https://doi.org/10.1158/2159-8290.CD-20-1598.
[82] J.M. Weiss, T. Csoszi, M. Maglakelidze, R.J. Hoyer, J.T. Beck, M. Domine Gomez, A. Lowczak, R. Aljumaily, C.M. Rocha Lima, R.V. Boccia, W. Hanna, P. Nikolinakos, V.K. Chiu, T.K. Owonikoko, S.R. Schuster, M.A. Hussein, D. A. Richards, P. Sawrycki, I. Bulat, J.T. Hamm, L.L. Hart, S. Adler, J.M. Antal, A. Y. Lai, J.A. Sorrentino, Z. Yang, R.K. Malik, S.R. Morris, P.J. Roberts, K. H. Dragnev, G1T28-02 Study Group. Myelopreservation with the CDK4/6 inhibitor trilaciclib in patients with small-cell lung cancer receiving first-line chemotherapy: a phase Ib/randomized phase II trial, Ann. Oncol. 30 (2019) 1613–1621, https://doi.org/10.1093/annonc/mdz278.
[83] K. Powell, V. Prasad, Concerning FDA approval of trilaciclib (Cosela) in extensive-stage small-cell lung cancer, Transl. Oncol. 14 (2021), 101206, https://doi.org/10.1016/j.tranon.2021.101206.
[84] C.A. Lipinski, F. Lombardo, B.W. Dominy, P.J. Feeney, Experimental and computational approaches to estimate solubility and permeability in drug discovery and development settings, Adv. Drug Deliv. Rev. 46 (2001) 3–26, https://doi.org/10.1016/s0169-409x(00)00129-0.
[85] A.L. Hopkins, C.R. Groom, A. Alex, Ligand efficiency: a useful metric for lead selection, Drug Discov. Today 9 (2004) 430–431, https://doi.org/10.1016/S1359-6446(04)03069-7.
[86] P.D. Leeson, B. Springthorpe, The influence of drug-like concepts on decision-making in medicinal chemistry, Nat. Rev. Drug Discov. 6 (2007) 881–890, https://doi.org/10.1038/nrd2445.
[87] S. Ekins, N.K. Litterman, C.A. Lipinski, B.A. Bunin, Thermodynamic proxies to compensate for biases in drug discovery methods, Pharm. Res. 33 (2016) 194–205, https://doi.org/10.1007/s11095-015-1779-y.
[88] A.L. Hopkins, G.M. Keserü, P.D. Leeson, D.C. Rees, C.H. Reynolds, The role of ligand efficiency metrics in drug discovery, Nat. Rev. Drug Discov. 13 (2014) 105–121, https://doi.org/10.1038/nrd4163.
[89] P.D. Leeson, Molecular inflation, attrition, and the rule of five, Adv. Drug Deliv. Rev. 101 (2016) 22–33, https://doi.org/10.1016/j.addr.2016.01.018.
[90] D.F. Veber, S.R. Johnson, H.Y. Cheng, B.R. Smith, K.W. Ward, K.D. Kopple, Molecular properties that influence the oral bioavailability of drug candidates, J. Med Chem. 45 (2002) 2615–2623, https://doi.org/10.1021/jm020017n.
[91] T.I. Oprea, Property distribution of drug-related chemical databases, J. Comput. Aided Mol. Des. 14 (2000) 251–264, https://doi.org/10.1023/a:1008130001697.
[92] P.D. Leeson, A.P. Bento, A. Gaulton, A. Hersey, E.J. Manners, C.J. Radoux, A. R. Leach, Target-based evaluation of "drug-like" properties and ligand efficiencies, J. Med Chem. 64 (2021) 7210–7230, https://doi.org/10.1021/acs.jmedchem.1c00416.
[93] J.J. Cui, M. McTigue, M. Nambu, M. Tran-Dubé, M. Pairish, H. Shen, L. Jia, H. Cheng, J. Hoffman, P. Le, M. Jalaie, G.H. Goetz, K. Ryan, N. Grodsky, Y. L. Deng, M. Parker, S. Timofeevski, B.W. Murray, S. Yamazaki, S. Aguirre, Q. Li, H. Zou, J. Christensen, Discovery of a novel class of exquisitely selective mesenchymal-epithelial transition factor (c-MET) protein kinase inhibitors and identification of the clinical candidate 2-(4-(1-(quinolin-6-ylmethyl)-1H-[1–3] triazolo[4,5-*b*]pyrazin-6-yl)-1H-pyrazol-1-yl)ethanol (PF-04217903) for the treatment of cancer, J. Med. Chem. 55 (2012) 8091–8109, https://doi.org/10.1021/jm300967g.
[94] S.H. Bertz, The first general index of molecular complexity, J. Am. Chem. Soc. 1103 (1981) 3559–3601.
[95] J.B. Hendrickson, P. Huang, A.G. Toczko, Molecular complexity: a simplified formula adapted to individual atoms, J. Chem. Inf. Comput Sci. 27 (1987) 63–67.
[96] T.J. Ritchie, S.J. Macdonald, Physicochemical descriptors of aromatic character and their use in drug discovery, J. Med. Chem. 57 (2014) 7206–7215, https://doi.org/10.1021/jm500515d.
[97] M.K. Bayliss, J. Butler, P.L. Feldman, D.V. Green, P.D. Leeson, M.R. Palovich, A. J. Taylor, Quality guidelines for oral drug candidates: dose, solubility and lipophilicity, Drug Discov. Today 21 (2016) 1719–1727, https://doi.org/10.1016/j.drudis.2016.07.007.
[98] T.I. Oprea, C.G. Bologa, S. Brunak, A. Campbell, G.N. Gan, A. Gaulton, S. M. Gomez, R. Guha, A. Hersey, J. Holmes, A. Jadhav, L.J. Jensen, G.L. Johnson, A. Karlson, A.R. Leach, A. Ma'ayan, A. Malovannaya, S. Mani, S.L. Mathias, M. T. McManus, T.F. Meehan, C. von Mering, D. Muthas, D.T. Nguyen, J. P. Overington, G. Papadatos, J. Qin, C. Reich, B.L. Roth, S.C. Schürer, A. Simeonov, L.A. Sklar, N. Southall, S. Tomita, I. Tudose, O. Ursu, D. Vidovic, A. Waller, D. Westergaard, J.J. Yang, G. Zahoránszky-Köhalmi, Unexplored therapeutic opportunities in the human genome, Nat. Rev. Drug Discov. 17 (2018) 377, https://doi.org/10.1038/nrd.2018.52.
[99] L. Huang, S. Jiang, Y. Shi, Tyrosine kinase inhibitors for solid tumors in the past 20 years (2001-2020), J. Hematol. Oncol. 13 (2020) 143, https://doi.org/10.1186/s13045-020-00977-0.
[100] K. Bechman, M. Yates, J.B. Galloway, The new entries in the therapeutic armamentarium: the small molecule JAK inhibitors, Pharm. Res. 147 (2019), 104392, https://doi.org/10.1016/j.phrs.2019.104392. Corrigendum doi: 10.1016/j.phrs.2020.104634.
[101] K. Bechman, G.B. Galloway, K.L. Winthrop, Small-molecule protein kinase inhibitors and the risk of fungal infections, Curr. Fungal Infect. Rep. (2019) 219–243.
[102] C.I. Wells, H. Al-Ali, D.M. Andrews, C.R.M. Asquith, A.D. Axtman, I. Dikic, D. Ebner, P. Ettmayer, C. Fischer, M. Frederiksen, R.E. Futrell, N.S. Gray, S. B. Hatch, S. Knapp, U. Lücking, M. Michaelides, C.E. Mills, S. Müller, D. Owen, A. Picado, K.S. Saikatendu, M. Schröder, A. Stolz, M. Tellechea, B.J. Turunen, S. Vilar, J. Wang, W.J. Zuercher, T.M. Willson, D.H. Drewry, The kinase chemogenomic set (KCGS): an open science resource for kinase vulnerability identification, Int. J. Mol. Sci. 22 (2021) 566, https://doi.org/10.3390/ijms22020566.
[103] J. Choo, G. Heo, C. Pothoulakis, E. Im, Posttranslational modifications as therapeutic targets for intestinal disorders, Pharm. Res. (2021), 105412, https://doi.org/10.1016/j.phrs.2020.105412.
[104] R. Roskoski Jr., Blockade of mutant RAS oncogenic signaling with a special emphasis on KRAS, Pharm. Res. 172 (2021), 105806, https://doi.org/10.1016/j.phrs.2021.105806.
[105] A. Cichońska, B. Ravikumar, R.J. Allaway, F. Wan, S. Park, O. Isayev, S. Li, M. Mason, A. Lamb, Z. Tanoli, M. Jeon, S. Kim, M. Popova, S. Capuzzi, J. Zeng, K. Dang, G. Koytiger, J. Kang, C.I. Wells, T.M. Willson, T.I. Opera, A. Schlessinger, D.H. Drewry, G. Stolovitzky, K. Wennerberg, J. Guinney, T. Aittokallio, IDG-DREAM drug-kinase binding prediction challenge consortium, Crowdsourced mapping of unexplored target space of kinase inhibitors, Nat. Commun. 12 (2021) 3307, https://doi.org/10.1038/s41467-021-23165-1.
[106] X. Lu, J.B. Smaill, K. Ding, New promise and opportunities for allosteric kinase inhibitors, Angew. Chem. Int Ed. Engl. 59 (2020) 13764–13776, https://doi.org/10.1002/anie.201914525.
[107] Roskoski R. Jr. Guidelines for preparing color figures for everyone including the colorblind. Pharmacol Res. 2017;119:240–1. doi: 10.1016/j.phrs.2017.02.005. Erratum in: Pharmacol Res. 2019;139:569. doi: ⟨10.1016/j.phrs.2018.09.019⟩.